

---

# 3D-SBDD meets LLM: Towards FDA-Level Drug Design

---

Bowen Gao<sup>\*12</sup> Yanwen Huang<sup>\*3</sup> Yiqiao Liu<sup>3</sup> Wenxuan Xie<sup>4</sup> Bowei He<sup>5</sup> Haichuan Tan<sup>1</sup> Wei-Ying Ma<sup>1</sup>  
Ya-Qin Zhang<sup>1</sup> Yanyan Lan<sup>16</sup>

## Abstract

Structure-guided molecular generation plays a key role in early drug discovery by designing compounds for specific protein targets. While recent 3D generative models improve docking scores, they often generate chemically implausible structures outside drug-like space. To address this, we introduce the Molecule Reasonable Ratio (MRR), a new metric for assessing structural plausibility. We propose the Collaborative Intelligence Drug Design (CIDD) framework, combining 3D interaction modeling with large language models (LLMs) and Chain-of-Thought reasoning. CIDD generates spatially compatible, drug-like, and synthesizable molecules. On the CrossDocked2020 benchmark, it improves metrics like QED, SA, and MRR, and raises the success rate—from 15.72% to 34.59%—by balancing binding affinity and drug-likeness, showing the power of integrating geometry with symbolic reasoning.

## 1. Introduction

Structure-based drug design (SBDD) enables the generation of compounds tailored to protein binding sites, and recent 3D generative models—such as autoregressive methods (e.g., AR (Luo et al., 2021), Pocket2Mol (Peng et al., 2022)) and diffusion-based approaches (e.g., TargetDiff (Guan et al., 2023), MolCRAFT (Qu et al., 2024))—have made notable progress. However, these models often produce chemically implausible structures, including overly fused

rings and unstable scaffolds (Figure 2a), which may boost docking scores but harm drug-likeness and stability.

To quantify this issue, we introduce the **Molecular Reasonability Ratio (MRR)**, which measures the fraction of chemically reasonable molecules relative to drug-like standards. Existing models show low MRRs (e.g., TargetDiff: 37.8%, MolCRAFT: 58.5%) compared to FDA-approved drugs (85.9%), revealing a major gap. While some models (e.g., TAGMol) incorporate drug-likeness optimization (e.g., QED (Bickerton et al., 2012)), they still underperform in overall reasonability. In contrast, LLMs (e.g., GPT-4) achieve high MRRs (97.5%) due to their broad chemical knowledge, but lack the spatial awareness for affinity-driven generation.

We propose **CIDD** (Collaborative Intelligence for Drug Design), a framework that integrates 3D generative models with large language models (LLMs) to combine geometric interaction modeling with chemical reasoning. Rather than generating final molecules, 3D models provide spatially meaningful proposals, which are refined through LLM-driven Chain-of-Thought (CoT) reasoning across specialized modules—*Interaction Analysis*, *Design*, *Reflection*, and *Selection*. This modular architecture enables interpretable, chemically plausible design aligned with medicinal chemistry workflows.

Evaluated on CrossDocked2020 (Francoeur et al., 2020), CIDD improves the overall success rate—from **15.72% to 34.59%**—while consistently enhancing QED, SA, MRR, and QikProp (Schrödinger, LLC, 2025) compliance.

### Key contributions:

- **Problem Identification:** We identify structural irrationality in 3D models and introduce MRR to quantify drug-like plausibility.
- **CIDD framework:** We present the first unified approach combining spatial modeling with LLM-based reasoning for molecule generation.
- **State-of-the-art results:** CIDD improves drug-likeness and affinity, demonstrating the power of collaborative AI in molecular design.

<sup>\*</sup>Equal contribution <sup>1</sup>Institute for AI Industry Research (AIR), Tsinghua University. <sup>2</sup>Department of Computer Science and Technology, Tsinghua University. <sup>3</sup>Department of Pharmaceutical Science, Peking University. <sup>4</sup>School of Future Technology, South China University of Technology. <sup>5</sup>Department of Computer Science, City University of Hong Kong. <sup>6</sup>Beijing Academy of Artificial Intelligence (BAAI). Correspondence to: Yanyan Lan <lanyanyan@air.tsinghua.edu.cn>.

## 2. Preliminaries

### 2.1. Structure-Based Drug Design

Structure-based drug design (SBDD) aims to generate molecules  $x$  that bind to a given protein pocket  $P$ . Recent deep generative methods include CVAE-based LiGAN (Ragoza et al., 2022), autoregressive models like AR (Luo et al., 2021) and Pocket2Mol (Peng et al., 2022), and diffusion models such as TargetDiff (Guan et al., 2023), IPDiff (Huang et al., 2024), and DecompDiff (Guan et al., 2024). TAGMol (Dorna et al., 2024) introduces gradient-based optimization during generation. Fragment-based approaches like DrugGPS (Zhang & Liu, 2023) and MolCRAFT (Qu et al., 2024) leverage modular representations or Bayesian flows. These methods typically produce intermediate 3D point clouds or graphs that are later converted into chemically valid molecules.

### 2.2. Large Language Models

Large language models (LLMs) such as GPT-4 (Achiam et al., 2023), LLaMA (Touvron et al., 2023), and ChatGLM (GLM et al., 2024) have shown strong capabilities in language, coding, and reasoning tasks. Their application to drug discovery is growing (Chakraborty et al., 2023), with models like ChatDrug (Liu et al., 2024) enabling molecular generation and editing via natural language. However, pocket-conditioned molecular design remains challenging, as LLMs struggle to capture complex 3D spatial and chemical features inherent in protein-ligand interactions—information that goes beyond what can be conveyed in pure textual form.

## 3. Methods

### 3.1. Evaluating the Gap Between Generated Molecules and Real Drugs

Drug-likeness is a multidimensional property representing the probability  $p(\text{drug})$  that a molecule reaches its biological target—an assessment distinct from binding affinity. Popular proxies such as QED (Bickerton et al., 2012) and Lipinski’s Rule of Five (Lipinski et al., 2012) face two key limitations. First, legacy bias: these metrics were calibrated on historical chemical space and often assign high scores to structurally implausible molecules produced by modern generative models. Second, oversimplification: QED uses only seven descriptors and poorly distinguishes molecules in DrugBank (Knox et al., 2024), whose average QED is below 0.5.

To address these limitations, we propose a two-tiered evaluation framework. The first tier, structural reasonability, assesses medicinal chemistry features such as aromaticity, ring stability, and hybridization consistency. The second tier

evaluates physicochemical and pharmacokinetic suitability through ADME/T-related descriptors. Together, these tiers offer a more robust evaluation of generative models by emphasizing both chemical plausibility and therapeutic relevance.

**Molecular Reasonability Ratio (MRR).** MRR is a rule-based metric designed to detect structural inconsistencies in generated molecules, particularly failures in ring conjugation that deviate from typical medicinal chemistry patterns. It analyzes hybridization states of ring atoms, excluding fully aromatic or fully saturated rings. After removing peripheral substituents, the molecule is flagged if the remaining ring atoms are neither uniformly  $sp^2$  nor  $sp^3$ . For example, partially conjugated rings such as cyclohexene or cyclohexa-1,3-diene are marked as unreasonable. Though not exhaustive, MRR provides interpretable, domain-informed filtering that complements valence checks and ADME-based screens. The full algorithm is described in Appendix F.

**QikProp Multiple Property Requirements.** We further evaluate molecular suitability using QikProp (Schrödinger, LLC, 2025), a predictive tool for drug-likeness based on properties such as solubility, lipophilicity, polar surface area, metabolic site count, and oral absorption (Ioakimidis et al., 2008). A molecule passes the evaluation only if all  $N$  predefined property constraints  $P_1, P_2, \dots, P_N$  are satisfied:

$$\text{QikProp} = \begin{cases} 1 & \text{if } P_1 \wedge P_2 \wedge \dots \wedge P_N \text{ are satisfied,} \\ 0 & \text{otherwise.} \end{cases}$$

### 3.2. Bridging the Gap with CIDD Framework

We propose the **Collaborative Intelligence Drug Design (CIDD)** framework (Figure 1), a modular system for target-specific molecule generation that combines 3D interaction modeling with LLM-guided refinement. CIDD consists of two stages: the **Structure-Based Interaction Generator (SBIG)**, which produces interaction-aware scaffolds, and the **LLM-Enhanced Drug Designer (LEDD)**, which refines them into viable compounds:

$$x_0 = \text{SBIG}(\text{Target}), \quad x = \text{LEDD}(x_0, \text{Target})$$

Here,  $x_0$  captures spatial compatibility, while LEDD leverages the reasoning capabilities of large language models to generate chemically valid molecules. Inspired by medicinal chemists’ workflows, CIDD formalizes a two-step design process that bridges 3D structural intent with drug-likeness.

#### 3.2.1. PIPELINE OVERVIEW

CIDD decomposes molecule generation into modular reasoning steps. SBIG first generates interaction-centric scaffold



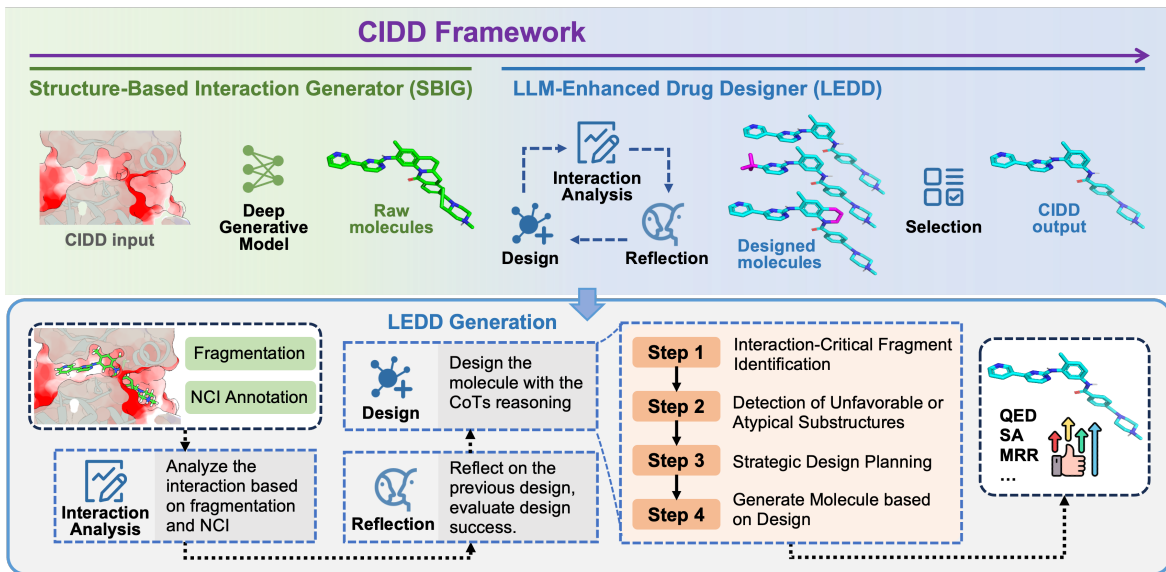


Figure 1. Overview of the CIDD framework. Top: end-to-end pipeline integrating SBIG and LEDD. Bottom: detailed view of LEDD’s LLM-based design process, which designs and generates molecules through interaction analysis, reflection, and Chain-of-Thought-driven reasoning.

folds, which are analyzed by the **Interaction Analysis Module** to extract fragment-level binding features. The **Design Module** then proposes optimized structures, guided by these interaction profiles. Each new molecule is evaluated, and the **Reflection Module** compares designs across iterations to inform refinement. Finally, the **Selection Module** identifies the optimal candidate based on interaction and drug-likeness criteria.

### 3.2.2. INTERACTION ANALYSIS MODULE

This module docks a candidate  $x_i$  into the protein pocket  $P$ , fragments it via BRICS (Degen et al., 2008), and detects key non-covalent interactions (e.g., hydrogen bonds,  $\pi$ - $\pi$  stacking). These features are summarized into an interaction profile  $I_i$  using a specialized language model:

$$\text{LLM}_I(x_i, P) \rightarrow I_i$$

The profile links molecular fragments to their roles in binding, guiding downstream design.

### 3.2.3. DESIGN MODULE

Given a scaffold  $x_0$ , its interaction profile  $I_0$ , and prior feedback  $R$ , the **Design Module** uses an LLM to output a refinement plan and new molecule:

$$\text{LLM}_D(x_0, I_0, R) \rightarrow (D_i, x_i)$$

To emulate real-world drug design workflows, we implement a **Chain-of-Thought** prompting strategy that guides the LLM through a domain-informed reasoning pipeline

with four sequential stages. **(1) Interaction-Critical Fragment Identification:** the model analyzes  $x_0$  and highlights fragments forming key non-covalent interactions with the target, based on  $I_0$ . **(2) Detection of Unfavorable or Atypical Substructures:** chemically undesirable fragments—such as synthetically inaccessible motifs, strained rings, or poor physicochemical regions—are flagged for replacement. **(3) Strategic Design Planning:** the model proposes modifications that improve chemical viability while preserving interaction and topology, often substituting problematic regions with pharmaceutically preferred alternatives. **(4) Candidate Molecule Generation:** a new structure  $x_i$  is generated based on the design plan, ensuring both target interaction and drug-like properties.

### 3.2.4. REFLECTION AND SELECTION MODULES

The *Reflection Module* compares the design  $x_i$  to the original input:

$$\text{LLM}_R(x_0, I_0, D_i, x_i, I_i) \rightarrow R_i$$

The *Selection Module* ranks all candidates  $\{x_1, \dots, x_N\}$  and selects the best:

$$\text{LLM}_S(\{(x_1, I_1), \dots, (x_N, I_N)\}) \rightarrow x_{\text{best}}$$

This ensures the final molecule balances interaction strength and chemical realism. Prompt examples are in Appendix E.

Table 1. **Test Results on CrossDocked2020.** We benchmark several evaluation metrics, including Vina docking score, QED, SA, MRR, success ratio, and QikProp pass ratio. We also report the average molecular weight. Performance ranking per column is color-coded as follows: **best**, **second-best**

Category	Method	Vina ↓	QED ↑	SA ↑	MRR ↑	Success ↑	QikProp ↑	MW
VAE-based	LiGAN	-6.640	0.394	0.601	59.08%	2.79%	17.37%	286.44
AR-based	AR	-6.737	0.507	0.635	56.67%	3.28%	18.66%	247.50
AR-based	Pocket2Mol	-7.246	<b>0.573</b>	<b>0.758</b>	<b>67.88%</b>	14.60%	29.58%	234.30
Diffusion-based	TargetDiff	-7.452	0.474	0.579	37.81%	3.04%	27.63%	346.24
Diff + Inter-Guide	IPDiff	-7.745	0.511	0.627	29.83%	5.31%	25.11%	328.34
Diff + Inter-Prior	DecompDiff	<b>-8.260</b>	0.444	0.609	62.60%	<b>15.72%</b>	29.04%	424.09
Diff + Multi-Guide	TAGMol	-7.563	0.563	0.583	37.31%	3.23%	<b>32.31%</b>	325.50
Fragment-based	DrugGPS	-7.396	0.463	0.622	54.80%	7.17%	25.60%	329.88
BFN-based	MolCRAFT	-7.783	0.503	0.685	58.47%	13.72%	22.37%	325.63
3DSBDD + LLM	CIDD	<b>-8.496</b>	<b>0.576</b>	<b>0.735</b>	<b>81.74%</b>	<b>34.59%</b>	<b>35.22%</b>	336.70

## 4. Experiments

### 4.1. Experiment Settings

**Dataset.** We follow 3D-SBDD protocols and use the Cross-Docked2020 dataset (Francoeur et al., 2020), adopting TargetDiff’s train/test split (Guan et al., 2023) with 100 protein pockets reserved for testing.

**Metrics.** We evaluate with standard metrics: Vina docking score (Trott & Olson, 2010), QED (Bickerton et al., 2012), SA score (Ertl & Schuffenhauer, 2009), and molecular diversity ( $1 - \text{ECFP4 similarity}$  (Rogers & Hahn, 2010)). As 3D conformations are not directly generated, Vina Score/Min is omitted. Beyond these, we assess drug potential using **MRR** (structural plausibility) and **QikProp pass ratio** (pharmacokinetic profiling). A molecule is counted as successful if it meets:  $\text{Vina} < -8.18$ ,  $\text{QED} > 0.25$ ,  $\text{SA} > 0.59$ , and passes molecular reasonability and QikProp filters (Long et al., 2022).

**Baselines.** CIDD is compared against diverse 3D generative models: VAE-based **LiGAN** (Ragoza et al., 2022), autoregressive **AR** (Luo et al., 2021) and **Pocket2Mol** (Peng et al., 2022), and diffusion-based **TargetDiff** (Guan et al., 2023), **IPDiff** (Huang et al., 2024), **DecompDiff** (Guan et al., 2024), **TAGMol** (Dorna et al., 2024), as well as fragment-based **DrugGPS** (Zhang & Liu, 2023) and flow-based **MolCRAFT** (Qu et al., 2024).

**CIDD Settings.** MolCRAFT is used for SBIG, with GPT-4o powering all LEDD modules. The Design Module proposes 5 candidates per round; one is selected. For each pocket, 10 molecules are generated. SBIG models use Cross-Docked2020 and pretrained weights.

### 4.2. General Results

As shown in Table 1, **CIDD** achieves strong and consistent performance across key drug-likeness metrics, including QED, MRR, SA, and QikProp pass ratio, while maintaining favorable binding affinity. Compared to baselines like **IPDiff** and **TAGMol**—which rely on predictor-guided sampling—CIDD shows superior MRR and overall balance. IPDiff improves docking scores but underperforms in MRR, and TAGMol, while boosting QED, lags in MRR and SA, suggesting overfitting to specific scoring functions.

CIDD’s advantage lies in combining the structural modeling strength of 3D generative models with the chemical reasoning capabilities of LLMs. By leveraging expert prompts and the LLM’s embedded domain knowledge, it generates candidates that are not only strong binders but also synthetically viable and pharmacologically realistic. This leads to a significantly higher success ratio of **34.59%**—more than double the best baseline (15.72%). Notably, CIDD produces molecules that are on average **50% larger** in molecular weight than Pocket2Mol (336.70 vs. 234.30), yet still achieves superior QED, SA, and docking scores. This indicates that CIDD’s performance is not due to metric overfitting via small molecules, but reflects genuine drug-likeness in more complex structures.

## 5. Conclusion

We presented **CIDD**, a collaborative framework that unifies 3D interaction modeling and LLM-driven reasoning for structure-based drug design. CIDD addresses a key limitation of current generative models: the tendency to generate interaction-compatible but chemically unreasonable molecules. Through a modular, interpretable generation process, CIDD achieves state-of-the-art results on

the CrossDocked2020 benchmark—substantially improving drug-likeness metrics (QED, SA, MRR, QikProp) while maintaining high binding affinity. By bridging 3D geometric modeling with language-guided design, our approach sets a foundation for future directions in rational, interpretable, and generalizable drug generation. We envision such a collaborative paradigm enabling broader tasks such as target discovery and hit-to-lead optimization in early-stage drug discovery.

## Acknowledgements

This work is supported by Beijing Academy of Artificial Intelligence (BAAI).

## References

- Achiam, J., Adler, S., Agarwal, S., Ahmad, L., Akkaya, I., Aleman, F. L., Almeida, D., Altenschmidt, J., Altman, S., Anadkat, S., et al. Gpt-4 technical report. *arXiv preprint arXiv:2303.08774*, 2023.
- Bickerton, G. R., Paolini, G. V., Besnard, J., Muresan, S., and Hopkins, A. L. Quantifying the chemical beauty of drugs. *Nature chemistry*, 4(2):90–98, 2012.
- Chakraborty, C., Bhattacharya, M., and Lee, S.-S. Artificial intelligence enabled chatgpt and large language models in drug target discovery, drug discovery, and development. *Molecular Therapy-Nucleic Acids*, 33:866–868, 2023.
- DeepSeek-AI, Liu, A., Feng, B., Xue, B., Wang, B., Wu, B., Lu, C., Zhao, C., Deng, C., Zhang, C., Ruan, C., Dai, D., Guo, D., Yang, D., Chen, D., Ji, D., Li, E., Lin, F., Dai, F., Luo, F., Hao, G., Chen, G., Li, G., Zhang, H., Bao, H., Xu, H., Wang, H., Zhang, H., Ding, H., Xin, H., Gao, H., Li, H., Qu, H., Cai, J. L., Liang, J., Guo, J., Ni, J., Li, J., Wang, J., Chen, J., Chen, J., Yuan, J., Qiu, J., Li, J., Song, J., Dong, K., Hu, K., Gao, K., Guan, K., Huang, K., Yu, K., Wang, L., Zhang, L., Xu, L., Xia, L., Zhao, L., Wang, L., Zhang, L., Li, M., Wang, M., Zhang, M., Zhang, M., Tang, M., Li, M., Tian, N., Huang, P., Wang, P., Zhang, P., Wang, Q., Zhu, Q., Chen, Q., Du, Q., Chen, R. J., Jin, R. L., Ge, R., Zhang, R., Pan, R., Wang, R., Xu, R., Zhang, R., Chen, R., Li, S. S., Lu, S., Zhou, S., Chen, S., Wu, S., Ye, S., Ye, S., Ma, S., Wang, S., Zhou, S., Yu, S., Zhou, S., Pan, S., Wang, T., Yun, T., Pei, T., Sun, T., Xiao, W. L., Zeng, W., Zhao, W., An, W., Liu, W., Liang, W., Gao, W., Yu, W., Zhang, W., Li, X. Q., Jin, X., Wang, X., Bi, X., Liu, X., Wang, X., Shen, X., Chen, X., Zhang, X., Chen, X., Nie, X., Sun, X., Wang, X., Cheng, X., Liu, X., Xie, X., Liu, X., Yu, X., Song, X., Shan, X., Zhou, X., Yang, X., Li, X., Su, X., Lin, X., Li, Y. K., Wang, Y. Q., Wei, Y. X., Zhu, Y. X., Zhang, Y., Xu, Y., Xu, Y., Huang, Y., Li, Y., Zhao, Y., Sun, Y., Li, Y., Wang, Y., Yu, Y., Zheng, Y., Zhang, Y., Shi, Y., Xiong, Y., He, Y., Tang, Y., Piao, Y., Wang, Y., Tan, Y., Ma, Y., Liu, Y., Guo, Y., Wu, Y., Ou, Y., Zhu, Y., Wang, Y., Gong, Y., Zou, Y., He, Y., Zha, Y., Xiong, Y., Ma, Y., Yan, Y., Luo, Y., You, Y., Liu, Y., Zhou, Y., Wu, Z. F., Ren, Z. Z., Ren, Z., Sha, Z., Fu, Z., Xu, Z., Huang, Z., Zhang, Z., Xie, Z., Zhang, Z., Hao, Z., Gou, Z., Ma, Z., Yan, Z., Shao, Z., Xu, Z., Wu, Z., Zhang, Z., Li, Z., Gu, Z., Zhu, Z., Liu, Z., Li, Z., Xie, Z., Song, Z., Gao, Z., and Pan, Z. Deepseek-v3 technical report, 2024. URL <https://arxiv.org/abs/2412.19437>.
- Degen, J., Wegscheid-Gerlach, C., Zaliani, A., and Rarey, M. On the art of compiling and using ‘drug-like’ chemical fragment spaces. *ChemMedChem*, 3(10):1503, 2008.
- Dorna, V., Subhalingam, D., Kolluru, K., Tuli, S., Singh, M., Singal, S., Krishnan, N., and Ranu, S. Tagmol: Target-aware gradient-guided molecule generation. *arXiv preprint arXiv:2406.01650*, 2024.
- Ertl, P. and Schuffenhauer, A. Estimation of synthetic accessibility score of drug-like molecules based on molecular complexity and fragment contributions. *Journal of cheminformatics*, 1:1–11, 2009.
- Francoeur, P. G., Masuda, T., Sunseri, J., Jia, A., Iovanisci, R. B., Snyder, I., and Koes, D. R. Three-dimensional convolutional neural networks and a cross-docked data set for structure-based drug design. *Journal of chemical information and modeling*, 60(9):4200–4215, 2020.
- GLM, T., Zeng, A., Xu, B., Wang, B., Zhang, C., Yin, D., Zhang, D., Rojas, D., Feng, G., Zhao, H., et al. Chatglm: A family of large language models from glm-130b to glm-4 all tools. *arXiv preprint arXiv:2406.12793*, 2024.
- Guan, J., Qian, W. W., Peng, X., Su, Y., Peng, J., and Ma, J. 3d equivariant diffusion for target-aware molecule generation and affinity prediction. *arXiv preprint arXiv:2303.03543*, 2023.
- Guan, J., Zhou, X., Yang, Y., Bao, Y., Peng, J., Ma, J., Liu, Q., Wang, L., and Gu, Q. Decompdiff: diffusion models with decomposed priors for structure-based drug design. *arXiv preprint arXiv:2403.07902*, 2024.
- Guo, D., Yang, D., Zhang, H., Song, J., Zhang, R., Xu, R., Zhu, Q., Ma, S., Wang, P., Bi, X., et al. Deepseek-r1: Incentivizing reasoning capability in llms via reinforcement learning. *arXiv preprint arXiv:2501.12948*, 2025.
- Huang, Z., Yang, L., Zhou, X., Zhang, Z., Zhang, W., Zheng, X., Chen, J., Wang, Y., Cui, B., and Yang, W. Protein-ligand interaction prior for binding-aware 3d molecule diffusion models. In *The Twelfth International Conference on Learning Representations*, 2024.

- Ioakimidis, L., Thoukydidis, L., Mirza, A., Naeem, S., and Reynisson, J. Benchmarking the reliability of qikprop. correlation between experimental and predicted values. *QSAR & Combinatorial Science*, 27(4):445–456, 2008.
- Knox, C., Wilson, M., Klinger, C. M., Franklin, M., Oler, E., Wilson, A., Pon, A., Cox, J., Chin, N. E., Strawbridge, S. A., et al. Drugbank 6.0: the drugbank knowledgebase for 2024. *Nucleic acids research*, 52(D1):D1265–D1275, 2024.
- Lipinski, C. A., Lombardo, F., Dominy, B. W., and Feeney, P. J. Experimental and computational approaches to estimate solubility and permeability in drug discovery and development settings. *Advanced drug delivery reviews*, 64:4–17, 2012.
- Liu, S., Wang, J., Yang, Y., Wang, C., Liu, L., Guo, H., and Xiao, C. Conversational drug editing using retrieval and domain feedback. In *The twelfth international conference on learning representations*, 2024.
- Long, S., Zhou, Y., Dai, X., and Zhou, H. Zero-shot 3d drug design by sketching and generating. *Advances in Neural Information Processing Systems*, 35:23894–23907, 2022.
- Luo, S., Guan, J., Ma, J., and Peng, J. A 3d generative model for structure-based drug design. *Advances in Neural Information Processing Systems*, 34:6229–6239, 2021.
- Peng, X., Luo, S., Guan, J., Xie, Q., Peng, J., and Ma, J. Pocket2mol: Efficient molecular sampling based on 3d protein pockets. In *International Conference on Machine Learning*, pp. 17644–17655. PMLR, 2022.
- Qu, Y., Qiu, K., Song, Y., Gong, J., Han, J., Zheng, M., Zhou, H., and Ma, W.-Y. Molcraft: Structure-based drug design in continuous parameter space. *arXiv preprint arXiv:2404.12141*, 2024.
- Ragoza, M., Masuda, T., and Koes, D. R. Generating 3d molecules conditional on receptor binding sites with deep generative models. *Chemical science*, 13(9):2701–2713, 2022.
- Rogers, D. and Hahn, M. Extended-connectivity fingerprints. *Journal of chemical information and modeling*, 50(5):742–754, 2010.
- Schrödinger, LLC. *QikProp*. Schrödinger, LLC, New York, NY, 2025. Schrödinger Release 2021-2.
- Touvron, H., Lavril, T., Izacard, G., Martinet, X., Lachaux, M.-A., Lacroix, T., Rozière, B., Goyal, N., Hambro, E., Azhar, F., et al. Llama: Open and efficient foundation language models. *arXiv preprint arXiv:2302.13971*, 2023.
- Trott, O. and Olson, A. J. Autodock vina: improving the speed and accuracy of docking with a new scoring function, efficient optimization, and multithreading. *Journal of computational chemistry*, 31(2):455–461, 2010.
- Zhang, Z. and Liu, Q. Learning subpocket prototypes for generalizable structure-based drug design. In *International Conference on Machine Learning*, pp. 41382–41398. PMLR, 2023.

## A. Problem in Current Model

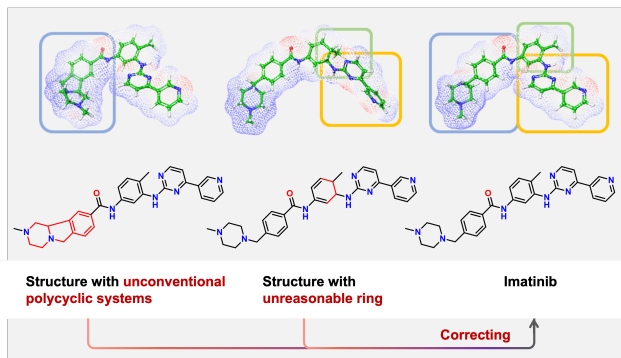


Figure 1. (a) **Common errors in 3D-SBDD outputs.** Minor structural changes can cause large deviations in 3D conformation, highlighting the challenge of correcting chemically uncommon structures without disrupting valid 3D shapes.

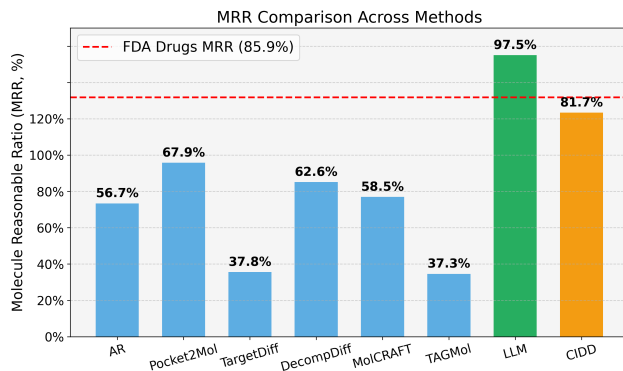


Figure 1. (b) **MRR comparison.** While FDA drugs reach 85.9% MRR, existing 3D models lag behind. LLM achieves 97.5%, and CIDD closes the gap with 81.7%.

Figure 2. Comparison of 3D generative model issues and MRR performance.

## B. Additional Experiment Results and Analysis

### B.1. Improvements with Different Models on Multiple Metrics

CIDD is a flexible framework designed to interface smoothly with a broad spectrum of 3D SBDD models, significantly enhancing the quality of generated molecules. As illustrated in Figure 4, CIDD brings substantial and consistent improvements across key drug-likeness metrics—including QED, SA Score, Reasonable Ratio, and QikProp Pass Ratio—achieving gains of 31.4%, 20.0%, 85.2%, and 102.8%, respectively. These improvements are observed across different base models, demonstrating CIDD’s strong generalization ability and its capacity to enhance diverse, diverse aspects of drug-likeness simultaneously. In contrast to optimization-based methods that often overfit individual metrics, CIDD drives broad and meaningful improvements that reflect a true advancement in the quality of generated drug candidates.

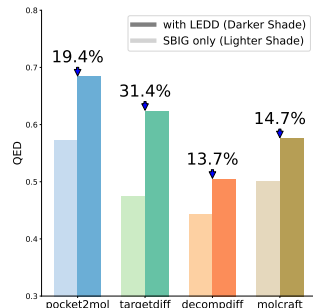


Figure 2. (a) QED

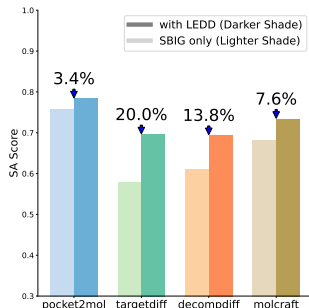


Figure 3. (b) SA Score

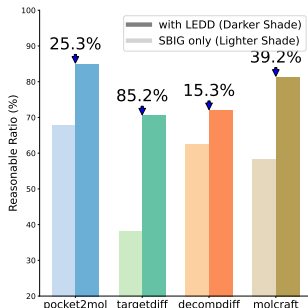


Figure 3. (c) Reasonable Ratio

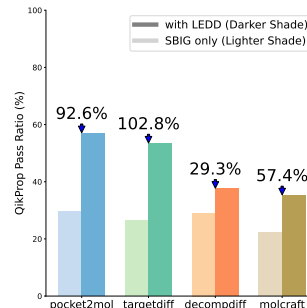


Figure 3. (d) QikProp Pass Ratio

Figure 4. Comparison of models using only SBIG outputs vs. CIDD (SBIG + LEDD), across various 3D-SBDD backbones and drug-likeness metrics.

### B.2. Ablation and Analysis

#### B.2.1. IMPACT OF DIFFERENT LLMs

We evaluate GPT-4o, GPT-4o-mini, DeepSeek-v3 (DeepSeek-AI et al., 2024), and DeepSeek-r1 (Guo et al., 2025) using MolCRAFT as the SBIG module (Table 2a). All models improve drug-likeness metrics (MRR, QikProp) and docking scores.

Table 2. Ablation studies on LLM variants and pure LLM-based SBDD.

Table 2. (a) Different LLM Backends in CIDD

LLM	Vina↓	MRR↑	Similarity↑
-	-7.78	58.47%	-
GPT-4o-mini	-8.29	80.02%	0.220
GPT-4o	-8.50	81.37%	0.296
DeepSeek-v3	-8.49	76.00%	0.379
DeepSeek-r1	-8.57	79.17%	0.182

Table 2. (b) LLM-Only vs. CIDD Comparison

	Vina↓	MRR↑	Success Ratio↑
LLM-SBDD	-6.244	97.45%	5.95%
CIDD-LLM	-7.230	90.97%	17.59%
CIDD	-8.496	81.74%	35.22%

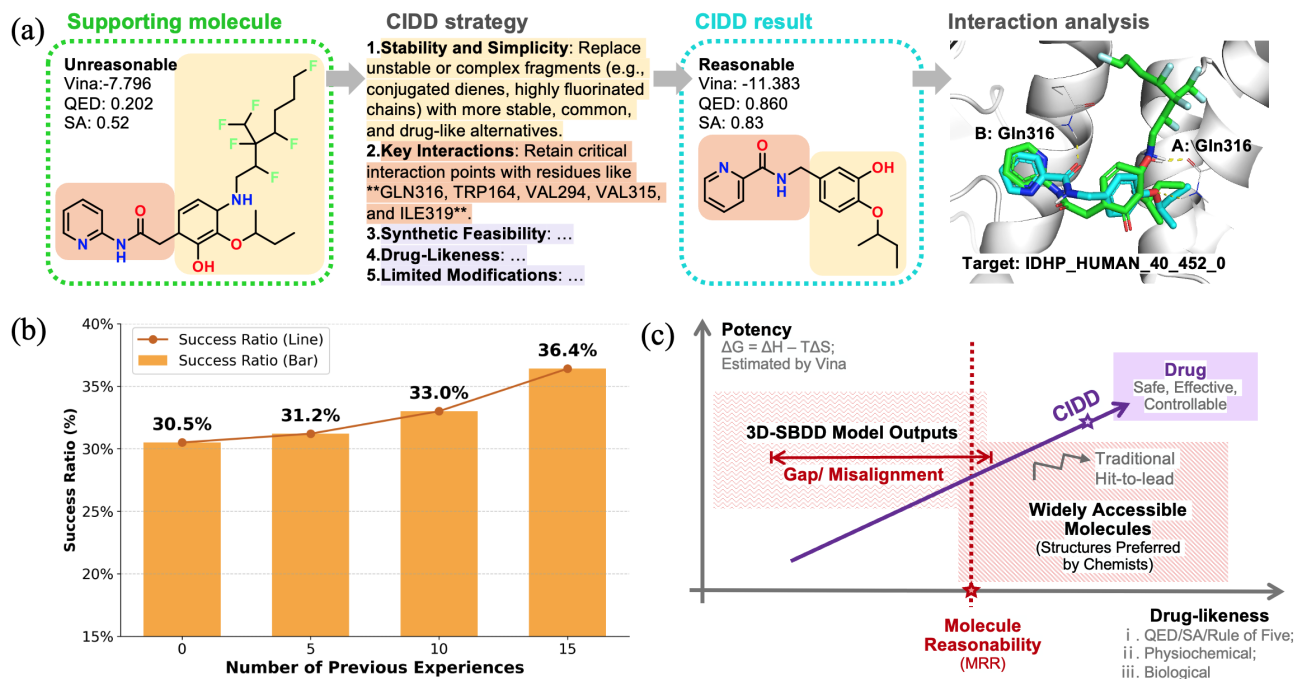


Figure 5. (a) A generation case and corresponding interpretable design strategy produced by CIDD, resulting in a structurally similar yet better compound. (b) CIDD demonstrates the ability to evolve by leveraging previous design experiences as context, improving generation success rates. (c) CIDD integrates the strengths of 3D-SBDD models and LLMs to enable practical drug design with both high potency and drug-likeness.

DeepSeek-v3 achieves property gains with minimal edits, while GPT-4o-mini struggles with similarity, and DeepSeek-r1 makes broader, less controllable changes. GPT-4o and DeepSeek-v3 best support CIDD’s goal of generating similar yet improved molecules. Smaller models like LLAMA-7B fail to follow design instructions. CIDD remains plug-and-play, benefiting from future LLM advances.

### B.2.2. USING PURE LLM FOR SBDD

LLMs alone struggle with 3D protein pocket interpretation in structure-based drug design (SBDD). To test this, we prompted an LLM with PDB-format pocket data and also evaluated CIDD-LLM, which uses LLM-SBDD within the CIDD framework. As shown in Table 2b, LLM-SBDD generates chemically reasonable molecules but performs poorly on binding affinity, leading to a lower success rate than standard CIDD. This highlights the need for combining 3D models’ interaction modeling with LLMs’ reasoning.



### B.3. Advantages and Impact of the CIDD Framework

**Interpretable Molecule Design.** Figure 5a illustrates the CIDD generation process. The LLM-powered modules analyze and refine the raw supporting molecule (green), producing a high-quality final structure (blue). Problematic fragments—such as an unreasonable diene or an uncommon fluorinated chain—are automatically identified and replaced (e.g., with a benzene ring), while side chains are adjusted to preserve key hydrogen bonds with Gln316 on both Chain A and B. These edits improve docking scores and enhance drug-relevant properties. CIDD performs this refinement through localized fragment substitutions, maintaining the core structure while improving overall drug potential. Notably, the process is inherently **interpretable**: each design step is traceable, with explicit rationales highlighting structural strengths and weaknesses. This transforms conventional opaque SBDD into a transparent, expert-assisting workflow. CIDD also enables the **automated creation of molecule pairs** that differ in drug-likeness with minimal structural edits. These pairs effectively capture how small chemical changes influence pharmaceutical viability, offering high-quality, distributionally aligned data for fine-tuning. Compared to random sampling, they provide more meaningful supervision and help mitigate data scarcity in 3D-SBDD (see Appendix I).

**Evolutionary Ability.** One key advantage of LLMs is their ability to leverage prior experience, provided as context, to generate insightful outputs. To illustrate this, we conducted a proof-of-concept experiment using a relatively lightweight LLM: GPT-4o-mini. The model was given varying numbers of previous design reports and results (0, 5, 10, and 15) as contextual input and tasked with generating insights to support the design module of CIDD. As shown in Figure 5b, the success rate improved as more prior reports were included. These results demonstrate CIDD’s capacity for continual evolution by incorporating accumulated experience—without requiring model retraining. This mirrors the way human experts enhance their performance through repeated exposure and practice.

**Generating Small Molecules with Both High Potency and Drug-Likeness.** Drug potential hinges on two key factors: potency and drug-likeness. While most 3D-SBDD models emphasize target fit, they often produce chemically unreasonable structures. As shown in Figure 5c, our **CIDD** framework bridges this gap by combining geometric modeling with LLM-driven reasoning. The LLM not only corrects unfavorable fragments but also plans coherent molecular edits that balance multiple objectives. By coordinating spatial and chemical constraints within a unified generation process, CIDD effectively overcomes the traditional trade-off between interaction strength and drug-likeness.

## C. Discussion on the Pharmaceutical Terminology

In this work, we employ a comprehensive set of evaluation metrics—**Vina**, **QED**, **SA**, our proposed **MRR**, the **Success Ratio**, and **QikProp**—to analyze different facets of molecular generation performance. Following established practices, we use Vina scores to assess the 3D complementarity between generated molecules and their target binding sites. Meanwhile, we evaluate broader molecular properties using standard metrics (QED and SA), the domain-informed MRR, and physicochemical and pharmacokinetic descriptors from QikProp, which are widely used in computer-aided drug design (CADD).

To clarify the key concepts underpinning our evaluation framework, we distinguish among **drug potential**, **drug-likeness**, **molecular reasonability**, and **chemical validity**.

Previous studies have often focused too narrowly on geometric complementarity, overlooking other essential requirements a drug-like molecule must fulfill. We introduce the term *drug potential* to describe the overall suitability of a molecule as a drug candidate, encompassing not only binding affinity but also synthetic accessibility, chemical stability, pharmacokinetics (absorption, distribution, metabolism, and excretion), and safety. These properties are intrinsically determined by molecular structure and collectively influence whether a molecule can reach its intended biological target and survive the drug development process.

The term *drug-likeness* is widely used in medicinal chemistry to reflect the multidimensional suitability of a molecule as a drug candidate. Drug discovery and development (DDD), however, are deeply influenced by human expertise—including implicit preferences for molecular scaffolds and nuanced, often tacit, domain knowledge that is difficult to formalize or quantify. As a result, even experienced medicinal chemists struggle to define or approximate the true probability function  $p(\text{drug})$ , which represents the likelihood that a molecule will become a viable therapeutic candidate. However, the machine learning community often oversimplifies *drug-likeness* to metrics such as QED or Lipinski’s Rule of Five, which capture only a narrow range of basic physicochemical properties. This simplification overlooks critical factors such as oral bioavailability, metabolic stability, and toxicity risks (e.g., hERG liability).

At a more fundamental level, a molecule must be *chemically valid*, meaning it adheres to basic chemical rules such as proper valence and atom types. However, we observe that many model-generated molecules—while technically valid—contain rare or unstable structural substructures that would be flagged by human medicinal chemists. These structures are neither common nor practically accessible and thus fall outside the bounds of what is typically accepted in pharmaceutical research. Despite the central importance of this distinction, prior work has not proposed an effective metric to differentiate between chemically plausible structures and those that are formally valid but unrealistic. To fill this gap, we propose MRR, a rule-based metric that reflects medicinal chemistry heuristics. It identifies implausible features such as unstable ring systems and uncommon conjugation patterns, offering an interpretable and practical means of identifying unrealistic model outputs.

By explicitly defining these concepts and introducing MRR, we aim to guide molecular generation efforts toward pharmaceutically meaningful directions, bridging the gap between computational outputs and real-world drug development feasibility.

## D. Limitations

One limitation of CIDD is its dependence on pretrained LLMs, which may occasionally introduce hallucinations in underexplored chemical regions.

## E. Detailed Prompts and Responses for LEDD

In this section, we present the detailed workflow of the CIDD framework, including the prompts and example responses for each module.

Figure 6 illustrates the complete drug design pipeline. The Interaction Module first identifies key fragments within the supporting molecule that interact with the protein pocket. This information is then utilized by the Design Module, which devises strategies to replace uncommon or unfavorable fragments while preserving crucial interactions. Once a new molecule is designed, the Evaluation Phase within the Design Module assesses its viability. Finally, the Reflection Module analyzes the design process and outcomes, highlighting both strengths and areas for improvement.

Figure 7 presents the prompt and example response for the Interaction Analysis Module.

Figures 8 and 9 display the prompt and example response for the Design Module.

Figures 10, 11, and 12 illustrate the prompt and example responses for the Reflection Module.

Figures 13 and 14 show the prompt and example response for the Selection Module.

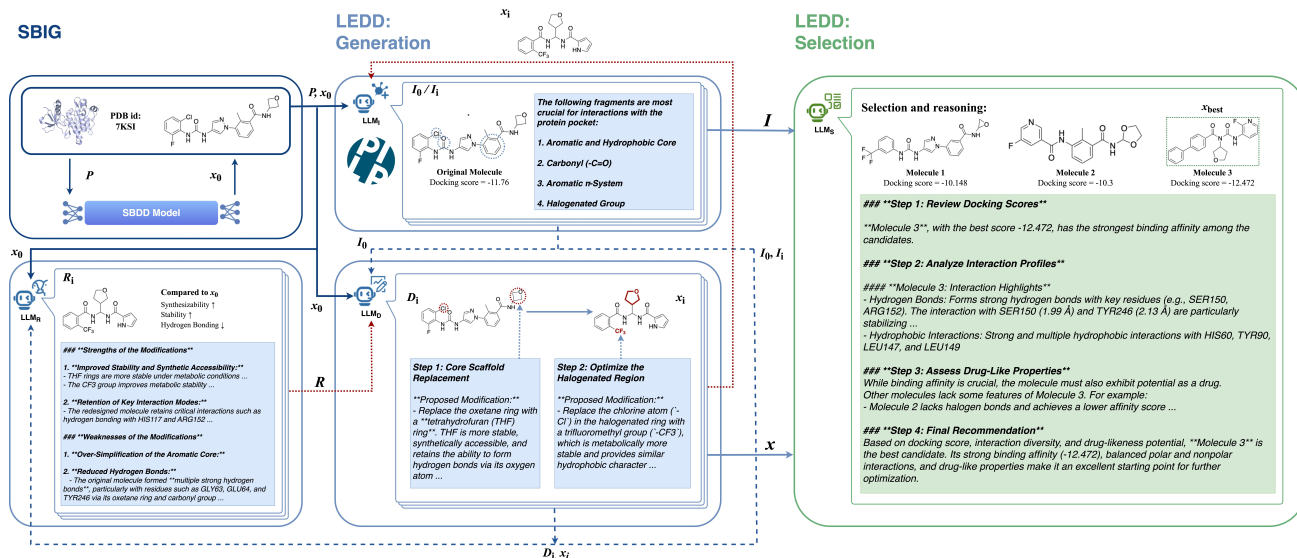


Figure 6. Workflow of CIDD framework



## Interaction analysis

The interaction analysis results are as follows: **[PLIP(Docking( $x_0$ , P))]**

The smiles string of the molecule is: **[ $x_0$ ]**

**[Important]** Using the information from the interaction analysis and the fragment labels, based on the coordinates matching, you need to identify the key fragment on the molecule that conduct the interaction with the protein pocket.

**[Important]** The format should be, which fragment can interact with which residue in the protein pocket. For example:

The fragment 'ethanol' can interact with the residue 'ASP123' in the protein pocket.

**[Important]** It should be at fragment level, instead of atom level. You need use the information from the fragment labels to identify which atom belongs to which fragment.



Query



LLM<sub>1</sub>

### Output [ $I_0$ ]:

#### ### **\*\*Key Fragments of Importance\*\***

Based on the analysis, the following fragments are most crucial for interactions with the protein pocket:

##### 1. **\*\*Aromatic and Hydrophobic Core:\*\***

- [C]C1=C[C]=[C][C]=C1 (Atoms: 5-11)
- Critical for hydrophobic interactions with ILE113, LEU142, and LEU147. This fragment anchors the molecule in the hydrophobic pocket.

##### 2. **\*\*Carbonyl (-C=O):\*\***

- Atoms `12, 13`
- Vital for hydrogen bonds, particularly with GLY63 and GLU64. This fragment contributes to the specificity of the interaction.

##### 3. **\*\*Oxetane Ring:\*\***

- [C]1[C][C]O1 (Atoms: 15-18)
- Key for hydrogen bonding with TYR246, providing excellent specificity and strength.

##### 4. **\*\*Aromatic $\pi$ -System:\*\***

- [C]1=NN[C]=C1 (Atoms: 0-4)
- Engaged in  $\pi$ -stacking with TYR90, stabilizing the ligand in the binding pocket.

##### 5. **\*\*Halogenated Group:\*\***

- FC1=CC(Cl)=[C][C]=[C]1 (Atoms: 23-30)
- Responsible for halogen bonding with PHE61, contributing to unique and specific interactions.

Figure 7. Interaction analysis module

## Design - Part 1

**[Instruction]**

This is the original molecule: **[X<sub>0</sub>]**

This is the interaction analysis: **[I<sub>0</sub>]**

Based on the interaction analysis, design modifications to the original molecule. Your job is scaffold hopping: change the core scaffold structure while retaining key pharmacophores.

**[Design Objectives]**

1. The modified molecule should be more stable and easier to synthesize than the original molecule. The new fragments should be common, stable and not weird.
2. The modified molecule should retain key properties of the original molecule, such as shape, size, and functionality.
3. The modified molecule should contain the key interaction types with the same residues as the original molecule.
4. The original molecule may contain uncommon or unstable fragments. Identify these fragments and replace them with more common and stable counterparts, ensuring that the modifications retain key properties of the original molecule, such as shape, size, and functionality. For instance, you might replace cyclohexadiene with benzene.
5. The modified molecule should be more like a drug candidate than the original molecule.

**[Design Requirements]**

1. Do not modify the molecule too much.
2. Please only give the modification steps, do not generate smiles by yourself. We will use another agent to generate the new molecule based on your design.

**[Experience Summary]**

We have done some modifications before. You can learn from the previous designs and reflections to make better modifications.

Here is the summary of the previous designs and reflections: **[R]**

Now, give us the modification suggestions and requirements.



Query



LLM<sub>D</sub>

**Output [D<sub>1</sub>]:****### \*\*Step 1: Core Scaffold Replacement\*\***

**\*\*Unstable or Uncommon Scaffold:\*\***

- The original scaffold contains an oxetane ring ('[C]1[C][C]O1'), which, while beneficial for solubility and hydrogen bonding, can be chemically unstable under metabolic conditions and is synthetically challenging.

**\*\*Proposed Modification:\*\***

- Replace the oxetane ring with a **\*\*tetrahydrofuran (THF) ring\*\***. THF is more stable, synthetically accessible, and retains the ability to form hydrogen bonds via its oxygen atom. Importantly, it maintains a similar size, shape, and polarity.

**### \*\*Step 2: Optimize the Halogenated Region\*\***

**\*\*Uncommon or Unstable Fragment:\*\***

- The halogenated aromatic fragment ('FC1=CC(Cl)=[C][C]=[C]1') can contribute to metabolic instability or toxicity (especially with chlorine) in some cases. The position and type of halogenation also determine interaction strength.

**\*\*Proposed Modification:\*\***

- Replace the chlorine atom ('-Cl') in the halogenated ring with a trifluoromethyl group ('-CF3'), which is metabolically more stable and provides similar hydrophobic character and electronic properties to maintain halogen-bonding interactions. The fluorine atom can remain unaltered.

**### \*\*Step 3: Revise the Aromatic Core\*\***

**\*\*Uncommon or Unstable Fragment:\*\***

- The core ring '[C]C1=C[C]=[C][C]=C1' is a polycyclic conjugated system prone to oxidative metabolism. While it provides hydrophobicity and anchors the molecule, replacing it with a more common aromatic fragment (e.g., phenyl) can reduce metabolic liabilities without compromising interactions.

**\*\*Proposed Modification:\*\***

- Replace '[C]C1=C[C]=[C][C]=C1' with **\*\*a phenyl ring (benzene)\*\***. Phenyl rings retain hydrophobicity and size while reducing the likelihood of oxidation and increasing synthetic accessibility.

Figure 8. Design Module

## Design - Part 2

Output [ $D_1$ ]:

## ### \*\*Step 4: Replace the 1,2,4-Triazine Ring\*\*

**\*\*Uncommon or Unstable Fragment:\*\***

- The [C]1=NN[C]=C1 (1,2,4-triazine ring) involved in  $\pi$ -stacking with TYR90 can be retained, but this structure is not very common in drug-like scaffolds and may pose synthetic challenges.

**\*\*Proposed Modification:\*\***

- Replace the 1,2,4-triazine ring with a **\*\*pyridine ring (C5H5N)\*\***. Pyridine maintains aromaticity and hydrogen bond acceptor potential (via the nitrogen atom) for  $\pi$ -stacking but is more drug-like and easier to synthesize.

## ### \*\*Step 5: Simplify Linker Chains\*\*

**\*\*Uncommon or Unstable Fragment:\*\***

- The linker fragment connecting the oxetane ring and other parts of the molecule may introduce unnecessary flexibility, which can lead to entropic penalties upon binding.

**\*\*Proposed Modification:\*\***

- Shorten the linker chain by removing or simplifying alkyl groups. Use fewer methylene groups where applicable to reduce flexibility while maintaining shape and size for proper binding.

## ### \*\*Summary of Modifications\*\*

1. **\*\*Oxetane Ring (Unstable/Uncommon):\*\*** Replace with **\*\*THF ring\*\*** to improve stability and synthetic accessibility while retaining hydrogen-bonding capability.
2. **\*\*Halogenated Aromatic Ring (Metabolic Liability):\*\*** Replace chlorine (`Cl`) with **\*\*trifluoromethyl group (`CF3`)\*\*** to improve metabolic stability while maintaining hydrophobic interactions and halogen bonding.
3. **\*\*Polycyclic Aromatic Core (Oxidative Risk):\*\*** Replace [C]C1=C[C]=[C][C]=C1 with a **\*\*phenyl ring (benzene)\*\*** to reduce metabolic liability while retaining hydrophobicity.
4. **\*\*1,2,4-Triazine Ring (Uncommon Scaffold):\*\*** Replace with a **\*\*pyridine ring\*\*** to retain  $\pi$ -stacking and hydrogen-bond acceptor potential while improving drug-likeness.
5. **\*\*Flexible Linkers (Entropic Penalty):\*\*** Simplify and rigidify linker regions by shortening alkyl chains, reducing flexibility.

This is the original molecule: [ $x_0$ ]

This is the modification designed by the design expert: [ $D_1$ ]

Change the molecule structure based on the modification designed by the design expert. Importantly, the modified molecule should be valid and make sense in the context of medicinal chemistry.

Now please only return the smiles string of the generated molecule. The smiles string should be enclosed in a pair of \$\$\$. For example: \$\$\$cccc\$\$\$



Query

Output [ $x_1$ ]:

\$\$\$C1=CC(C(F)(F)F)=C(C(=O)NC(CCCOC2)NC(=O)C3=CC=CN3)C=C1\$\$\$

Figure 9. Design Module

## Reflection - Part 1

**[Instruction]**

=====

This is the original molecule structure:  $[x_0]$

This is the interaction analysis of this molecule and the protein pocket:  $[I_0]$

=====

This is the modification design generated by you:  $[D_1]$

This is the molecule structure designed based on your modification:  $[x_1]$

This is the interaction analysis generated by interaction export agent:  $[I_1]$

Previously, we asked you to modify a molecule to get a new molecule that binds better to the protein pocket. We analyzed the binding of the new molecule to the protein pocket and put it together with the binding before the modification for comparison.

Based on these analyses, you need to reflect on the previous modification and provide feedback on the design. Besides, we hope you can find out which fragments inside the structure of these two molecules are useful for binding to the protein pocket.

=====

Please use critical thinking to analyze, pointing out both the good and the bad points. Your reflection is:



Query

LLM<sub>R</sub>**Output  $[R_1]$ :****### \*\*Strengths of the Modifications\*\*****1. \*\*Improved Stability and Synthetic Accessibility:\*\***

- Replacing the **oxetane ring** with a **tetrahydrofuran (THF) ring** is a commendable adjustment. THF rings are more stable under metabolic conditions, while retaining key hydrogen-bonding interactions and similar steric bulk. This was a sensible change that aligns well with drug-likeness principles.
- Removing the **chlorine atom** in favor of a **trifluoromethyl (CF<sub>3</sub>) group** was another thoughtful modification. The CF<sub>3</sub> group improves metabolic stability and reduces potential toxicity from reactive halogens, while maintaining the original hydrophobicity and shape.

**2. \*\*Retention of Key Interaction Modes:\*\***

- The redesigned molecule retains critical interactions such as hydrogen bonding with HIS117 and ARG152, hydrophobic interactions with HIS60, LEU147, and PHE188, and  $\pi$ -stacking with TYR90. These interactions are crucial for binding affinity and ensure the molecule continues to engage the protein pocket effectively.
- The **pyridine ring** (replacing the less common 1,2,4-triazine ring) aligns better with drug-likeness rules while maintaining hydrogen bonding and hydrophobic capabilities. This substitution strengthens the molecule's pharmacokinetic prospects.

**3. \*\*Refinement of Scaffolds and Simplification:\*\***

- Simplifying the polycyclic aromatic core into a **benzene ring** was a reasonable modification to reduce oxidation-prone elements. This ensures the molecule is more stable and synthetically tractable without losing significant hydrophobic interactions.

**### \*\*Weaknesses of the Modifications\*\*****1. \*\*Reduction in Docking Score:\*\***

- The docking score decreased from **-11.76 (original molecule)** to **-9.215 (modified molecule)**, indicating a clear drop in binding affinity. While the modified molecule retains key interactions, some critical binding contributions were inadvertently weakened during redesign. The TEF reduction suggests a loss of key complementary contacts between the ligand and protein pocket.

**2. \*\*Over-Simplification of the Aromatic Core:\*\***

- Replacing the conjugated aromatic system ( $[C]C1=C[C]=[C][C]=C1$ ) with a simple **benzene ring** reduced the hydrophobic surface area and  $\pi$ -electron system available for interactions. Consequently, hydrophobic interactions with residues like TYR90, ILE113, and LEU142 were diminished, and the molecule lost some of its ability to stabilize key  $\pi$ -interactions within the pocket.

**3. \*\*Unutilized Potential of the Trifluoromethyl Group:\*\***

- While the trifluoromethyl (CF<sub>3</sub>) group improved metabolic stability, it did not directly contribute to binding interactions within the protein pocket. This functional group occupies space but does not engage with any specific residues, effectively adding to molecular weight without enhancing binding. A better-placed or functionally active replacement could have yielded greater interaction strength.



## Reflection - Part 2

Output [ $R_1$ ]:4. **Reduced Hydrogen Bonds:**

- The original molecule formed **multiple strong hydrogen bonds**, particularly with residues such as GLY63, GLU64, and TYR246 via its oxetane ring and carbonyl group. These hydrogen bonds were either weakened or lost in the redesign, with new hydrogen bonds (forming with HIS117 and ARG152) failing to fully compensate for this depletion.

5. **Flexibility in the THF Ring:**

- While the THF ring is more stable than the oxetane ring, it likely introduces greater flexibility due to its sp<sup>3</sup>-hybridized carbons. This flexibility may lead to entropic penalties upon binding, making the molecule less efficient in achieving a preorganized, bioactive conformation.

6. **Over-Reliance on Hydrophobic Interactions:**

- Similar to the original molecule, the modified structure still relies heavily on **hydrophobic interactions** for binding (e.g., HIS60, TYR90, LEU147). Hydrophobic interactions are less specific than polar or ionic interactions, which are critical for selectivity and affinity. By not introducing additional polar groups, the redesign missed an opportunity to improve overall binding specificity.

### **Comparison of Binding Fragments**#### **Original Molecule:**1. **Oxetane Ring (Lost in the Redesign):**

- Forms key hydrogen bonds with TYR246 in the binding pocket, contributing significantly to specific and strong ligand binding. Its removal weakened overall binding affinity.

2. **Conjugated Hydrophobic Core ([C]C1=C[C]=[C][C]=C1):**

- Provides extensive hydrophobic and  $\pi$ -stacking interactions with residues such as ILE113, LEU142, and TYR90. Replacing this rich aromatic structure with a benzene ring reduced the hydrophobic and  $\pi$ -electron contribution to binding.

3. **Halogenated Aromatic Ring (FC1=CC(Cl)=[C][C]=[C]1):**

- Engages the protein via halogen bonding with PHE61, adding specificity to binding interactions. Replacing chlorine with CF<sub>3</sub> abolished some halogen bonds, weakening protein-ligand complementarity.

#### **Modified Molecule:**1. **THF Ring (Introduced):**

- Retains the ability to form hydrogen bonds (e.g., with ARG152). However, its introduction has caused greater flexibility and entropic penalties that may offset its stabilizing contributions.

2. **Trifluoromethyl Group (CF<sub>3</sub>, Introduced):**

- Metabolically stable and hydrophobic but does not directly interact with the protein. Its placement on the aromatic ring adds molecular weight but no functional enhancement to binding.

3. **Pyridine Ring (Introduced):**

- Maintains hydrogen-bonding with HIS117 and interacts hydrophobically with HIS60, performing well as a replacement for 1,2,4-triazine. Though not as inherently diverse in interaction opportunities as its predecessor, it improves the drug-likeness of the molecule.

4. **Benzene Ring (Simplified):**

- While it retains some hydrophobic interaction capability, this fragment no longer engages residues like TYR90 or PHE188 as robustly as the original conjugated aromatic system. This reduced binding affinity.

Figure 11. Reflection Module

## Reflection - Part 3

LLM<sub>R</sub>**Output [ $R_1$ ]:****### \*\*Key Fragments Retained or Lost for Binding\*\*****\*\*Critical Retained Fragments:\*\***

1. **\*\*Pyridine Ring\*\*** for  $\pi$ -stacking and hydrogen bonding with TYR90 and HIS117.
2. **\*\*Hydrogen Bonding Carbonyl Group\*\*** interacting with HIS117 and ARG152.

**\*\*Critical Fragments Lost:\*\***

1. **\*\*Oxetane Ring\*\*** contributed unusually strong hydrogen bonds to TYR246, which were lost in the redesign.
2. **\*\*Conjugated Hydrophobic Core\*\*** ensured multisite hydrophobic interactions and  $\pi$ -stacking with residues like LEU142 and TYR90.
3. **\*\*Halogenated Aromatic Ring\*\*** provided halogen bonds with PHE61, contributing unique specificity lost in the redesign.

**### \*\*Suggestions for Improvement\*\*****1. \*\*Reintroduce Hydrogen Bonding Groups:\*\***

- Add back polar fragments (e.g., hydroxyl, amide groups) to increase hydrogen-bonding capacity with residues like TYR246, GLY63, and GLU64.

**2. \*\*Revisit the Aromatic Core:\*\***

- Instead of oversimplifying the hydrophobic core to benzene, consider a polycyclic aromatic or heterocyclic system to balance hydrophobicity and metabolic stability.

**3. \*\*Optimize Trifluoromethyl Group Placement:\*\***

- Move or replace the CF<sub>3</sub> group with a fragment that directly engages residues in the protein pocket (e.g., a difluorophenyl or hydrophilic substituent).

**4. \*\*Rigidify the THF Ring:\*\***

- Lock the THF ring into a constrained system (e.g., fused bicyclic rings) to reduce flexibility and entropic penalties.

**### \*\*Conclusion\*\***

The modifications resulted in a molecule that is synthetically and metabolically improved but less effective in binding to the protein pocket, as indicated by the diminished docking score. While retaining important interactions, the redesign lost too many advantageous fragments (e.g., oxetane, conjugated aromatic core). Future optimizations should aim to restore lost interactions, improve hydrogen bonding, and balance hydrophobicity with polar contacts for stronger and more specific binding.

Figure 12. Reflection Module

## Selection - Part 1

**[Instruction]**

Given a protein pocket and a number of different molecules, I need you to find a molecule that is best suited to bind this protein pocket. We will provide you with interaction reports for each molecule and protein pocket and ask you to make choices based on this information. You should consider both the binding analysis and whether the molecule has potential to be a real drug. You should output the reason and the smiles string of the chosen molecule. The smiles string should be enclosed in a pair of \$\$\$\$. For example: ... (The reason) The chosen smiles is: \$\$\$CCO\$\$\$



Query

This is the molecule structure: [x<sub>n</sub>]

This is the interaction analysis of this molecule and the protein pocket: [I<sub>n</sub>]

=====

This is the molecule structure: [x<sub>m</sub>]

This is the interaction analysis of this molecule and the protein pocket: [I<sub>m</sub>]

=====

This is the molecule structure: [x<sub>p</sub>]

This is the interaction analysis of this molecule and the protein pocket: [I<sub>p</sub>]

=====

Please think step by step:



LLMs

**The chosen molecule is:**

O=C(C1=CC=C(C=C1)C2=CC=CC=C2)N(C3CCOC3)C(NC4=C(F)N=CC=C4)=O

The docking score of the chosen molecule is: -12.472

The reason for choosing the molecule is: To select the best molecule for binding to the protein pocket, we will step through the following considerations:

**### \*\*Step 1: Review Docking Scores\*\***

The docking score is a key metric indicating the binding affinity between a molecule and the protein pocket. Lower docking scores (more negative values) suggest stronger binding. The docking scores for the respective molecules are as follows:

1. Molecule 1: -10.148
2. Molecule 2: -10.3
3. Molecule 3: -12.472

From this, **Molecule 3**, with the best score of **-12.472**, has the strongest binding affinity among the candidates.

**### \*\*Step 2: Analyze Interaction Profiles\*\***

Building off the docking scores, we now consider the rich interaction profiles of each molecule. A molecule that forms diverse interactions will often bind more robustly and specifically to the protein pocket.

**#### \*\*Molecule 3: Interaction Highlights\*\***

- **Hydrophobic Interactions:** Strong and multiple hydrophobic interactions with HIS60, TYR90, LEU147, and LEU149, anchored by the aromatic benzene ring.
- **Hydrogen Bonds:** Forms strong hydrogen bonds with key residues (e.g., SER150, ARG152). The interaction with SER150 (1.99 Å) and TYR246 (2.13 Å) are particularly stabilizing.
- **π-Stacking:** Strong π-stacking with TYR90 (T-shaped geometry).
- **π-Cation Interactions:** Robust π-cation interaction with ARG152 (3.85 Å), stabilized further by ideal offset alignment (1.32 Å).
- **Halogen Bonds:** Two halogen bonds with GLU189 (3.84 Å) and ASN237 (3.40 Å) provide an additional layer of interaction, making this molecule unique in its interaction diversity.

Figure 13. Selection Module

## Selection - Part 2

**\*\*Key Strengths:\*\***

- The interaction diversity and strength of Molecule 3 far surpass other molecules, leveraging hydrophobic forces, hydrogen bonding,  $\pi$ -stacking,  $\pi$ -cation interactions, and halogen bonding.
- The molecule effectively anchors itself to both polar and nonpolar regions, ensuring specificity for the protein pocket.

**### \*\*Step 3: Assess Drug-Like Properties\*\***

While binding affinity is crucial, the molecule must also exhibit potential as a drug.

Properties relevant to drug-likeness include:

- **\*\*Hydrophobic Components:\*\*** Ensure solubility and stability for membrane diffusion.
- **\*\*Hydrogen Bonding Groups:\*\*** Contribute to specificity and bioactivity.
- **\*\*Halogen Incorporation:\*\*** Enhances membrane permeability and metabolic stability.
- **\*\*Compact, Non-Bulky Structure:\*\*** Ensures the molecule fits within the protein pocket without steric clashes.

For Molecule 3:

- The combination of aromatic rings, amide groups, and fluorine atoms supports balanced hydrophobic and polar properties, increasing stability and bioavailability.
- The inclusion of halogens enhances drug-likeness further.

Other molecules lack some features of Molecule 3. For example:

- Molecule 2 lacks halogen bonds and achieves a lower affinity score.
- Molecule 1 have good binding but lack the breadth of interactions seen with Molecule 3.

**### \*\*Step 4: Final Recommendation\*\***

Based on docking score, interaction diversity, and drug-likeness potential, **\*\*Molecule 3\*\*** is the best candidate. Its strong binding affinity (-12.472), balanced polar and nonpolar interactions, and drug-like properties make it an excellent starting point for further optimization.

**### \*\*Chosen Molecule\*\***

**\*\*Reason:\*\*** Molecule 3 exhibits the highest docking score, with diverse interaction types (hydrophobic, hydrogen bonding,  $\pi$ -stacking,  $\pi$ -cation, and halogen bonding) that secure it in critical regions of the protein pocket. Additionally, it offers promising drug-like features such as halogen incorporation and a well-optimized molecular structure.

**\*\*Selected SMILES String:\*\***

\$\$\$O=C(C1=CC=C(C=C1)C2=CC=CC=C2)N(C3CCOC3)C(NC4=C(F)N=CC=C4)=O\$\$\$

Figure 14. Selection Module

## F. Algorithm for MRR and AUR

The complete calculation process for assessing the reasonability of a molecule is outlined in Algorithm 1.



**Algorithm 1:** Evaluation of Molecular Reasonability**Input:** Molecule object (*mol*)**Output:** Molecular Reasonability (*MRR*) and Atom Unreasonable Ratio (*AUR*)**Step 1: Detect Carbonyl and Imine Group Carbons**Initialize an empty list for *carbonyl/imine carbons*.**foreach** *bond* in *mol* **do**
**if** *bond* is double and one atom is carbon, the other is oxygen or nitrogen **then**  
   Record the carbon atom in *carbonyl/imine groups*.
**Step 2: Identification of Ring Systems**Identify all ring structures and their corresponding atom indices within *mol*.

Calculate the number of atoms in each ring.

**foreach** *ring* in the molecule **do**
**if** the ring shares one or more atoms with another ring **then**  
   Group the connected rings into a single *ring system*.
**Step 3: Evaluation of Molecular Reasonability**

Exclude any atoms previously identified as part of carbonyl or imine groups.

Classify the remaining carbon atoms in each ring system as follows:

- *sp*<sup>2</sup> hybridized: Aromatic or unsaturated carbons.
- Non-*sp*<sup>2</sup> hybridized: Saturated carbons.

**foreach** *ring system* in the ring systems **do**
**if** the ring system contains multiple rings and all carbon atoms are non-*sp*<sup>2</sup> **then**  
   Mark the molecule as unreasonable.  
   Add the atoms to the unreasonable atom list.
**foreach** *ring system* in the remaining ring systems **do****foreach** *ring* in the ring system **do**
**if** all carbon atoms within the ring are consistent in hybridization (either all *sp*<sup>2</sup> or all non-*sp*<sup>2</sup>) **then**  
   Mark the ring as reasonable.
**else**

Add the ring to the remaining ring list.

**while** the remaining ring list is not empty **do****foreach** *ring* in the remaining ring list **do**

Exclude atoms that have already been classified as reasonable.

**if** all remaining carbon atoms are consistent in hybridization (either all *sp*<sup>2</sup> or all non-*sp*<sup>2</sup>) **then**  
   Mark the ring as reasonable.
**if** no new reasonable rings are identified **then**

Mark the molecule as unreasonable.

Add the carbon atoms in the remaining rings to the unreasonable atom list.

**Exit the loop.**Calculate *AUR* as the ratio of unreasonable atom count to the total ring atom count.**Return** *MRR* and *AUR*.**G. QikProp properties**

The full set of properties used for the QikProp pass ratio analysis is presented in Table 3.

The QikProp filter applied in the main text incorporates a comprehensive range of criteria provided by QikProp, including "#stars", "#amine", "#amidine", "#acid", "#amide", "#rotor", "#rtvFG", "mol\_MW", "dipole", "SASA", "FOSA", "FISA", "PISA", "WPSA", "volume", "donorHB", "accptHB", "dip<sup>2</sup>/V", "ACxDN:5/SA", "glob", "QPpolrz", "QPlogPC16", "QPlogPoct", "QPlogPw", "QPlogPo/w", "QPlogS", "CIQPlogS", "QPPCaco", "QPlogBB", "QPPMDCK", "QPlogKp", "IP(eV)", "EA(eV)", "#metab", "QPlogKhsa", "PercentHumanOralAbsorption", "SAFluorine", "SAamideO", "PSA", "#NandO", and "RuleOfThree".

Table 3. QikProp Properties and Descriptors

Property or Descriptor	Description	Range or Recommended Values
Molecule name	The molecule's identifier derived from the title line in the input structure file. If no title is provided, the file name is used.	
#stars	Count of descriptors or properties falling outside the 95% range for known drugs. A higher count indicates reduced drug-likeness.	0 – 5
#amine	Total non-conjugated amine groups present in the molecule.	0 – 1
#amidine	Number of amidine or guanidine functional groups in the structure.	0
#acid	Quantity of carboxylic acid groups in the molecule.	0 – 1
#amide	Count of non-conjugated amide groups.	0 – 1
#rotor	Number of rotatable bonds that are neither trivial nor sterically hindered.	0 – 15
#rtvFG	Total reactive functional groups present in the molecule, potentially affecting stability or toxicity.	0 – 2
mol.MW	Molecular weight of the compound.	130.0 – 725.0
Dipole	Calculated dipole moment of the molecule in Debye units.	1.0 – 12.5
SASA	Solvent-accessible surface area (SASA) in square angstroms, measured with a probe of 1.4 Å radius.	300.0 – 1000.0
FOSA	Hydrophobic part of the SASA, representing saturated carbon and attached hydrogen atoms.	0.0 – 750.0
FISA	Hydrophilic fraction of the SASA, encompassing polar atoms like nitrogen and oxygen.	7.0 – 330.0
PISA	SASA component attributable to $\pi$ -systems.	0.0 – 450.0
WPSA	Weakly polar component of the SASA, including atoms like halogens, phosphorus, and sulfur.	0.0 – 175.0
Volume	Total solvent-accessible volume in cubic angstroms, determined with a 1.4 Å radius probe.	500.0 – 2000.0
donorHB	Estimated number of hydrogen bonds donated to water in solution.	0.0 – 6.0
accpHB	Estimated number of hydrogen bonds accepted from water.	2.0 – 20.0
Dip <sup>2</sup> /V	Dipole moment squared divided by molecular volume, a key factor in solvation energy.	0.0 – 0.13
ACxDN <sup>0.5</sup> /SA	Cohesive interaction index in solids based on molecular properties.	0.0 – 0.05
glob	Descriptor measuring how close the shape of a molecule is to a sphere.	0.75 – 0.95
QPolrz	Predicted molecular polarizability in cubic angstroms.	13.0 – 70.0
QPlogPC16	Predicted partition coefficient between hexadecane and gas phases.	4.0 – 18.0
QPlogPoct	Predicted partition coefficient between octanol and gas phases.	8.0 – 35.0
QPlogPw	Predicted partition coefficient between water and gas phases.	4.0 – 45.0
QPlogPo/w	Predicted partition coefficient between octanol and water phases.	-2.0 – 6.5
QPlogS	Predicted solubility of the molecule in water (log S, in mol/L).	-6.5 – 0.5
CIQlogS	Conformation-independent prediction of water solubility (log S).	-6.5 – 0.5
QPPCaco	Predicted permeability through Caco-2 cells, in nm/s.	<25 poor, >500 great
QPlogBB	Predicted partition coefficient for brain/blood.	-3.0 – 1.2
QPPMDCK	Predicted permeability through MDCK cells, in nm/s.	<25 poor, >500 great
QPlogKp	Predicted skin permeability (log Kp).	-8.0 – -1.0
IP(eV)	Ionization potential calculated using PM3.	7.9 – 10.5
EA(eV)	Electron affinity calculated using PM3.	-0.9 – 1.7
#metab	Predicted number of possible metabolic reactions.	1 – 8
QPlogKhsa	Predicted binding affinity to human serum albumin.	-1.5 – 1.5
HumanOralAbsorption	Qualitative assessment of oral absorption: 1 (low), 2 (medium), or 3 (high).	
PercentHumanOralAbsorption	Quantitative prediction of oral absorption percentage.	>80% high, <25% poor
SAFluorine	Solvent-accessible fluorine surface area.	0.0 – 100.0
SAamideO	Solvent-accessible surface area of amide oxygen atoms.	0.0 – 35.0
PSA	Polar surface area, calculated for nitrogen, oxygen, and carbonyl groups.	7.0 – 200.0
#NandO	Total count of nitrogen and oxygen atoms.	2 – 15
RuleOfFive	Number of Lipinski's Rule of Five violations.	Max 4
RuleOfThree	Number of Jorgensen's Rule of Three violations.	Max 3
#ringatoms	Count of atoms within molecular rings.	
#in34	Number of atoms in 3- or 4-membered rings.	
#in56	Number of atoms in 5- or 6-membered rings.	
#noncon	Number of ring atoms unable to form conjugated aromatic systems.	
#nonHatm	Count of heavy (non-hydrogen) atoms in the structure.	
Jm	Predicted maximum transdermal transport rate ( $\mu\text{g cm}^{-2} \text{ hr}^{-1}$ ).	

## H. More Experiment Results

Based on the different criteria presented in Table 3, we provide additional pass ratio results in Table 4.

Filter 1 is identical to the QikProp filter used in the main text.

Filter 2 removes some non-essential properties and focuses on well-defined physicochemical properties, including "rtvFG", "QPlogS", "QPlogPo/w", "mol\_MW", "dipole", "SASA", "FOSA", "FISA", "IP(eV)", "EA(eV)", "#metab", "PercentHumanOralAbsorption", and "PSA".

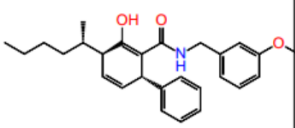
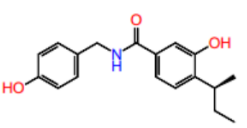
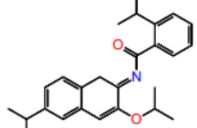
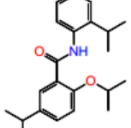
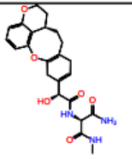
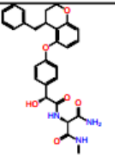
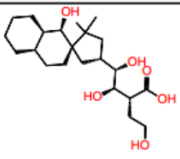
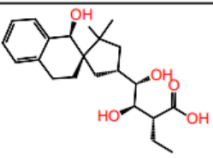
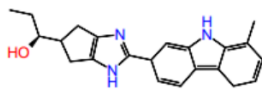
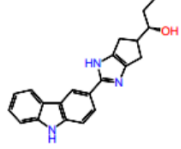
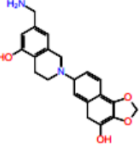
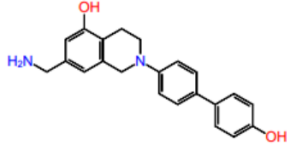
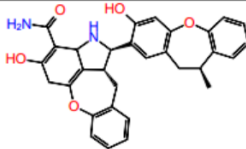
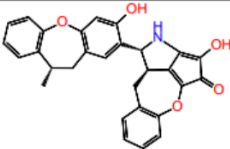
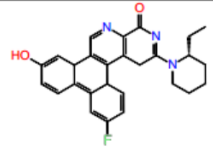
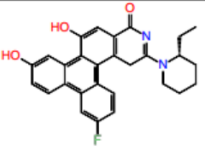
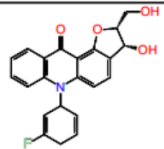
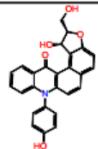
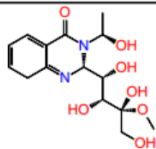
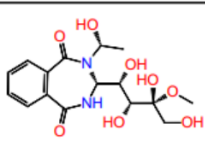
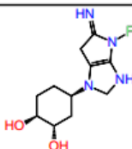
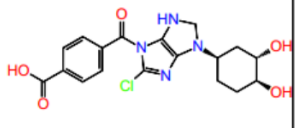
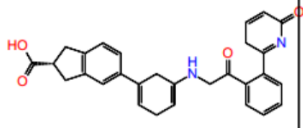
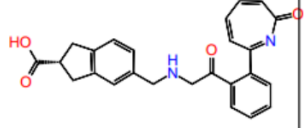
Filter 3 assesses molecular compliance with the "RuleOfFive" criterion. However, instead of allowing up to four violations as typically recommended, this filter adopts a stricter definition, considering only molecules that fully comply (i.e., setting the maximum allowable violations to zero).

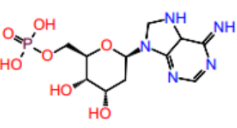
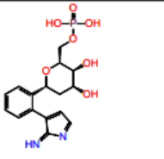
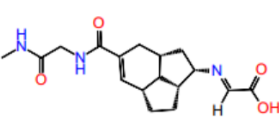
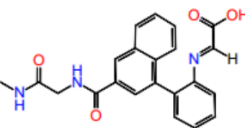
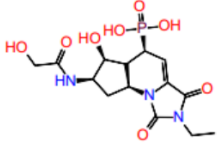
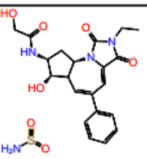
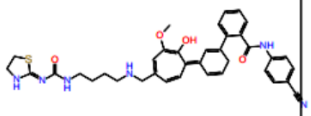
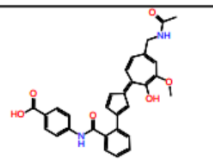
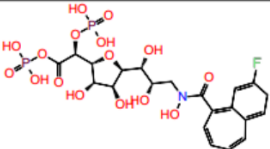
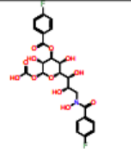
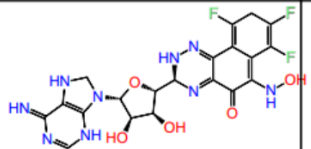
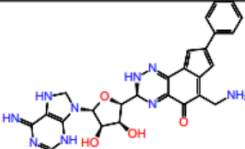
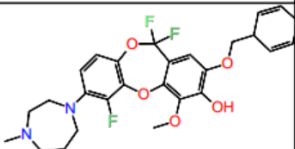
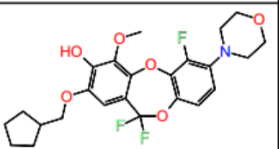
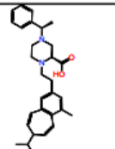
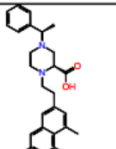
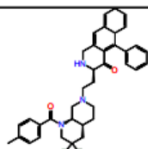
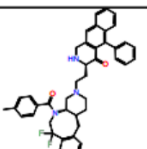
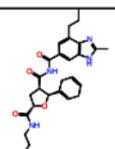
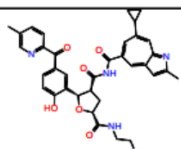
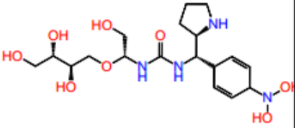
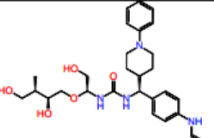
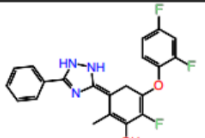
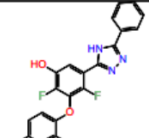
Table 4. QikProp results for different methods with and without CIDD

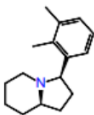
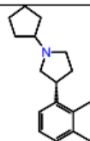
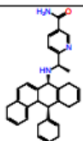
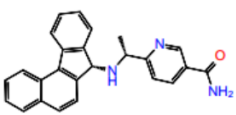
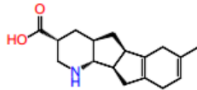
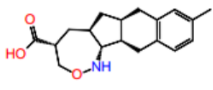
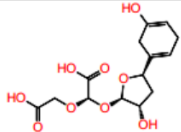
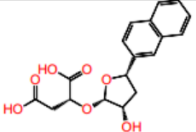
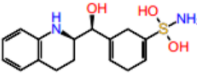
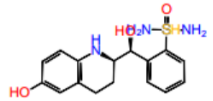
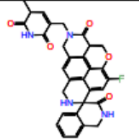
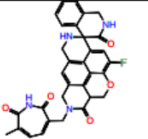
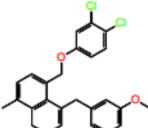
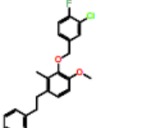
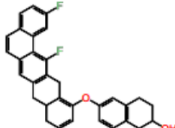
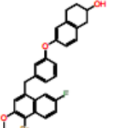
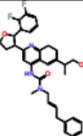
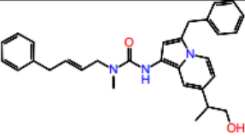
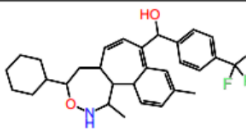
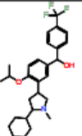
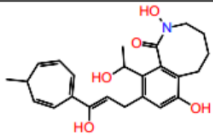
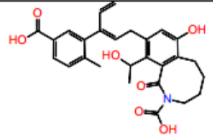
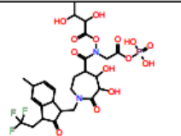
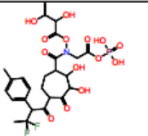
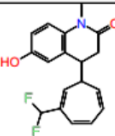
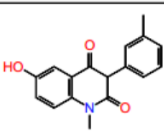
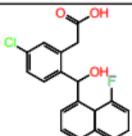
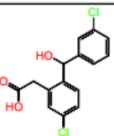
Method	Filter 1	Filter 2	Filter 3
<b>Pocket2Mol</b>			
Original	29.58%	51.52%	89.58%
CIDD	56.97%	75.64%	92.24%
<b>TargetDiff</b>			
Original	26.32%	48.20%	69.47%
CIDD	53.37%	75.60%	81.85%
<b>DecompDiff</b>			
Original	29.04%	53.96%	55.14%
CIDD	37.54%	68.48%	65.64%
<b>MolCRAFT</b>			
Original	22.37%	43.52%	66.45%
CIDD	35.22%	63.23%	74.09%

## I. More cases

More generated molecules from CIDD are presented below. For each case, we display the initial supporting molecule derived from 3D-SBDD models alongside the final designed molecules produced by CIDD.

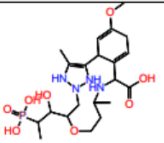
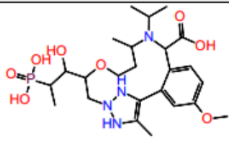
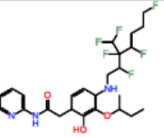
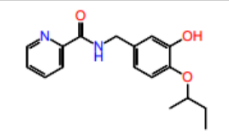
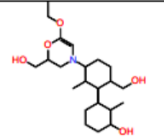
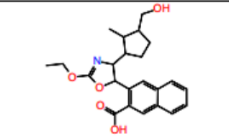
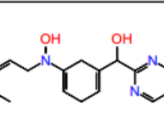
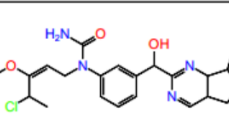
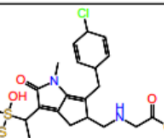
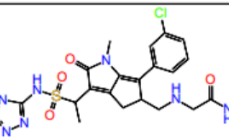
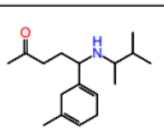
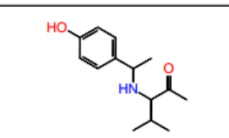
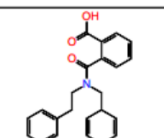
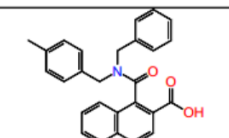
Supporting molecule	CIDD output	Supporting molecule	CIDD output
			
title: IDHP_HUMAN_40_452_0 : Unreasonable vina: -7.824	title: IDHP_HUMAN_40_452_0 : Reasonable vina: -10.106	title: IDHP_HUMAN_40_452_0 : Unreasonable vina: -7.941	title: IDHP_HUMAN_40_452_0 : Reasonable vina: -9.66
			
title: NOS1_HUMAN_302_723_0 : Unreasonable vina: -9.415	title: NOS1_HUMAN_302_723_0 : Reasonable vina: -10.098	title: NOS1_HUMAN_302_723_0 : Unreasonable vina: -8.054	title: NOS1_HUMAN_302_723_0 : Reasonable vina: -8.432
			
title: NOS1_HUMAN_302_723_0 : Unreasonable vina: -10.069	title: NOS1_HUMAN_302_723_0 : Reasonable vina: -10.22	title: NOS1_HUMAN_302_723_0 : Unreasonable vina: -9.287	title: NOS1_HUMAN_302_723_0 : Reasonable vina: -9.6
			
title: ABL2_HUMAN_274_551_0 : Unreasonable vina: -10.007	title: ABL2_HUMAN_274_551_0 : Reasonable vina: -10.946	title: ABL2_HUMAN_274_551_0 : Unreasonable vina: -9.916	title: ABL2_HUMAN_274_551_0 : Reasonable vina: -10.509
			
title: AK1BA_HUMAN_1_316_0 : Unreasonable vina: -10.421	title: AK1BA_HUMAN_1_316_0 : Reasonable vina: -10.778	title: NQO1_HUMAN_2_274_0 : Unreasonable vina: -8.37	title: NQO1_HUMAN_2_274_0 : Reasonable vina: -9.24
			
title: NQO1_HUMAN_2_274_0 : Unreasonable vina: -7.951	title: NQO1_HUMAN_2_274_0 : Reasonable vina: -9.51	title: PHP_SULSO_1_314_0 : Unreasonable vina: -11.034	title: PHP_SULSO_1_314_0 : Reasonable vina: -11.397

Supporting molecule	CIDD output	Supporting molecule	CIDD output
 <p>title: PHKG1_RABIT_6_296_ATPsite_0 : Unreasonable vina: -8.548</p>	 <p>title: PHKG1_RABIT_6_296_ATPsite_0 : Reasonable vina: -8.727</p>	 <p>title: BGL07_ORYSJ_25_504_0 : Unreasonable vina: -8.041</p>	 <p>title: BGL07_ORYSJ_25_504_0 : Reasonable vina: -9.949</p>
 <p>title: CD38_HUMAN_44_300_0 : Unreasonable vina: -7.443</p>	 <p>title: CD38_HUMAN_44_300_0 : Reasonable vina: -8.863</p>	 <p>title: TNKS2_HUMAN_948_1162_0 : Unreasonable vina: -10.284</p>	 <p>title: TNKS2_HUMAN_948_1162_0 : Reasonable vina: -10.974</p>
 <p>title: P2Y12_HUMAN_1_342_0 : Unreasonable vina: -10.463</p>	 <p>title: P2Y12_HUMAN_1_342_0 : Reasonable vina: -10.674</p>	 <p>title: HMD_METJA_1_358_0 : Unreasonable vina: -9.259</p>	 <p>title: HMD_METJA_1_358_0 : Reasonable vina: -10.458</p>
 <p>title: SQHC_ALIAD_1_631_0 : Unreasonable vina: -14.278</p>	 <p>title: SQHC_ALIAD_1_631_0 : Reasonable vina: -17.408</p>	 <p>title: SQHC_ALIAD_1_631_0 : Unreasonable vina: -13.626</p>	 <p>title: SQHC_ALIAD_1_631_0 : Reasonable vina: -13.825</p>
 <p>title: BGAT_HUMAN_63_353_0 : Unreasonable vina: -7.891</p>	 <p>title: BGAT_HUMAN_63_353_0 : Reasonable vina: -9.201</p>	 <p>title: CHIB_SERMA_1_499_0 : Unreasonable vina: -10.676</p>	 <p>title: CHIB_SERMA_1_499_0 : Reasonable vina: -13.113</p>
 <p>title: CHIB_SERMA_1_499_0 : Unreasonable vina: -7.115</p>	 <p>title: CHIB_SERMA_1_499_0 : Reasonable vina: -8.719</p>	 <p>title: NR1H4_HUMAN_258_486_0 : Unreasonable vina: -10.038</p>	 <p>title: NR1H4_HUMAN_258_486_0 : Reasonable vina: -11.021</p>

Supporting molecule	CIDD output	Supporting molecule	CIDD output
 <p>title: SDIA_ECOLI_1_171_0 : Unreasonable vina: -11.019</p>	 <p>title: SDIA_ECOLI_1_171_0 : Reasonable vina: -11.294</p>	 <p>title: SDIA_ECOLI_1_171_0 : Unreasonable vina: -8.52</p>	 <p>title: SDIA_ECOLI_1_171_0 : Reasonable vina: -13.937</p>
 <p>title: GSTP1_HUMAN_2_210_0 : Unreasonable vina: -7.591</p>	 <p>title: GSTP1_HUMAN_2_210_0 : Reasonable vina: -8.725</p>	 <p>title: HDHA_ECOLI_1_255_0 : Unreasonable vina: -7.709</p>	 <p>title: HDHA_ECOLI_1_255_0 : Reasonable vina: -8.778</p>
 <p>title: HDHA_ECOLI_1_255_0 : Unreasonable vina: -8.5</p>	 <p>title: HDHA_ECOLI_1_255_0 : Reasonable vina: -8.515</p>	 <p>title: NOS1_HUMAN_302_723_0 : Unreasonable vina: -11.943</p>	 <p>title: NOS1_HUMAN_302_723_0 : Reasonable vina: -12.979</p>
 <p>title: IDHP_HUMAN_40_452_0 : Unreasonable vina: -8.176</p>	 <p>title: IDHP_HUMAN_40_452_0 : Reasonable vina: -10.774</p>	 <p>title: NR1H4_HUMAN_258_486_0 : Unreasonable vina: -6.824</p>	 <p>title: NR1H4_HUMAN_258_486_0 : Reasonable vina: -8.578</p>
 <p>title: IDHP_HUMAN_40_452_0 : Unreasonable vina: -7.605</p>	 <p>title: IDHP_HUMAN_40_452_0 : Reasonable vina: -11.661</p>	 <p>title: CPXB_BACMB_2_464_0 : Unreasonable vina: -9.607</p>	 <p>title: CPXB_BACMB_2_464_0 : Reasonable vina: -10.132</p>
 <p>title: AK1BA_HUMAN_1_316_0 : Unreasonable vina: -9.845</p>	 <p>title: AK1BA_HUMAN_1_316_0 : Reasonable vina: -9.981</p>	 <p>title: P2Y12_HUMAN_1_342_0 : Unreasonable vina: -7.75</p>	 <p>title: P2Y12_HUMAN_1_342_0 : Reasonable vina: -16.253</p>
 <p>title: OLIAC_CANSA_1_101_0 : Unreasonable vina: -7.631</p>	 <p>title: OLIAC_CANSA_1_101_0 : Reasonable vina: -8.866</p>	 <p>title: SIR3_HUMAN_117_398_0 : Unreasonable vina: -8.238</p>	 <p>title: SIR3_HUMAN_117_398_0 : Reasonable vina: -8.331</p>

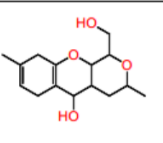
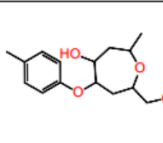
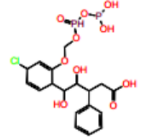
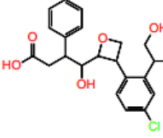
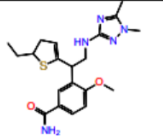
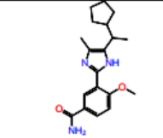
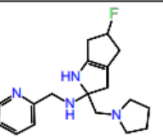
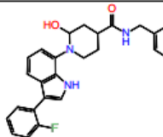
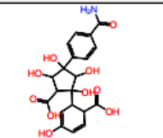
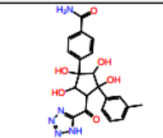
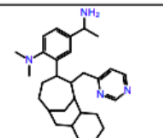
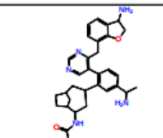
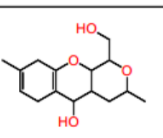
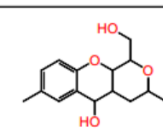
## Supporting molecule

## CIDD output

	
title: MCCF_ECOLDX_1_344_0 : Unreasonable vina: -8.726	title: MCCF_ECOLDX_1_344_0 : Reasonable vina: -8.947
	
title: IDHP_HUMAN_40_452_0 : Unreasonable vina: -7.796	title: IDHP_HUMAN_40_452_0 : Reasonable vina: -11.383
	
title: AKT1_HUMAN_1_137_0 : Unreasonable vina: -8.605	title: AKT1_HUMAN_1_137_0 : Reasonable vina: -9.926
	
title: HMD_METJA_1_358_0 : Unreasonable vina: -7.825	title: HMD_METJA_1_358_0 : Reasonable vina: -8.55
	
title: SIR3_HUMAN_117_398_0 : Unreasonable vina: -7.93	title: SIR3_HUMAN_117_398_0 : Reasonable vina: -10.435
	
title: DYRK2_HUMAN_145_550_0 : Unreasonable vina: -7.961	title: DYRK2_HUMAN_145_550_0 : Reasonable vina: -8.399
	
title: DIDH_RAT_1_319_0 : Unreasonable vina: -9.165	title: DIDH_RAT_1_319_0 : Reasonable vina: -10.631

## Supporting molecule

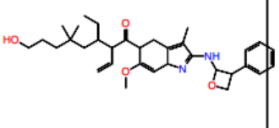
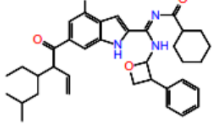
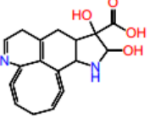
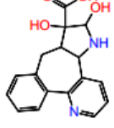
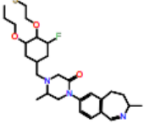
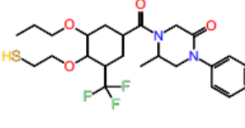
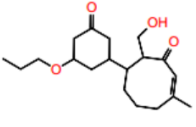
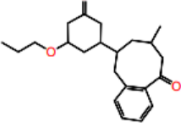
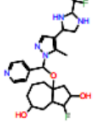
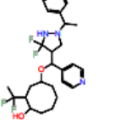
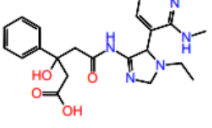
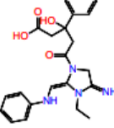
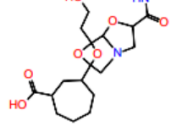
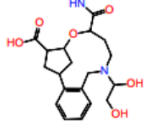
## CIDD output

	
title: DIDH_RAT_1_319_0 : Unreasonable vina: -8.26	title: DIDH_RAT_1_319_0 : Reasonable vina: -8.722
	
title: COAA_MYCTU_1_312_0 : Unreasonable vina: -7.572	title: COAA_MYCTU_1_312_0 : Reasonable vina: -8.731
	
title: M3K14_HUMAN_321_678_0 : Unreasonable vina: -7.453	title: M3K14_HUMAN_321_678_0 : Reasonable vina: -9.209
	
title: CHIB1_ASPFM_39_433_0 : Unreasonable vina: -8.054	title: CHIB1_ASPFM_39_433_0 : Reasonable vina: -10.096
	
title: SIR3_HUMAN_117_398_0 : Unreasonable vina: -6.991	title: SIR3_HUMAN_117_398_0 : Reasonable vina: -10.758
	
title: NOS3_HUMAN_65_480_0 : Unreasonable vina: -9.583	title: NOS3_HUMAN_65_480_0 : Reasonable vina: -10.652
	
title: DIDH_RAT_1_319_0 : Unreasonable vina: -8.503	title: DIDH_RAT_1_319_0 : Reasonable vina: -8.895



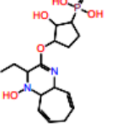
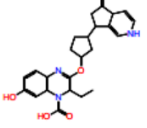
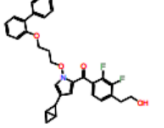
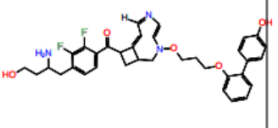
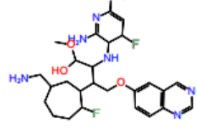
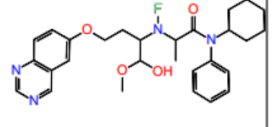
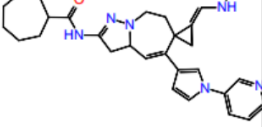
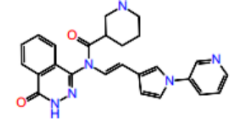
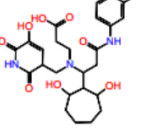
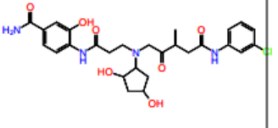
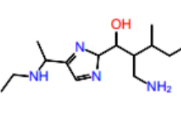
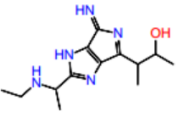
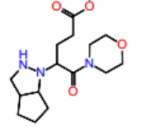
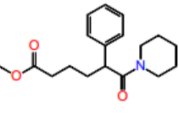
## Supporting molecule

## CIDD output

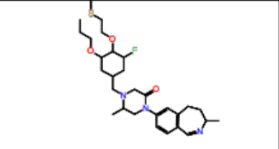
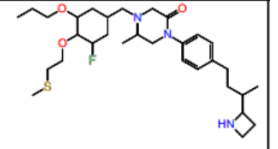
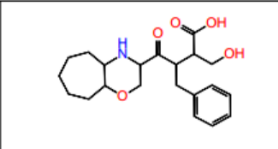
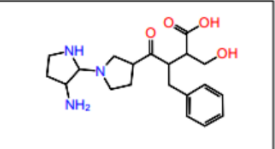
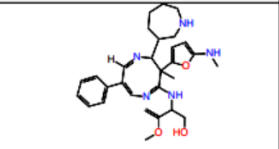
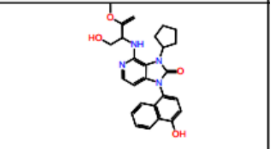
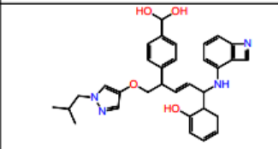
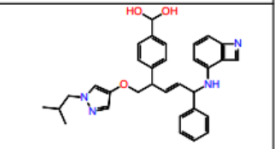
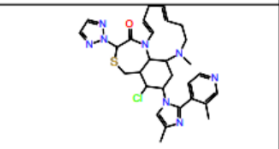
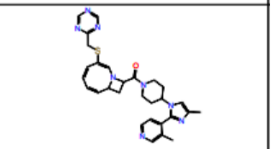
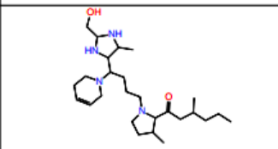
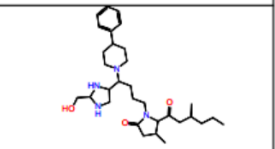
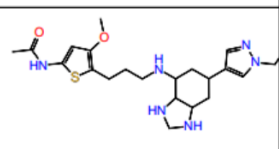
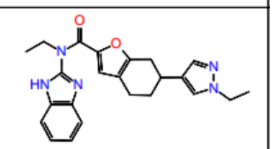
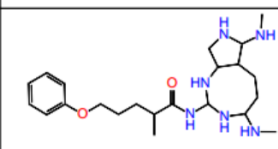
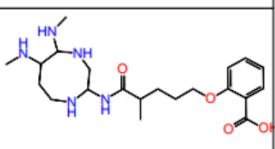
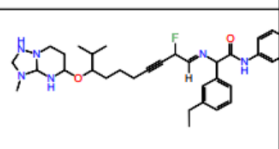
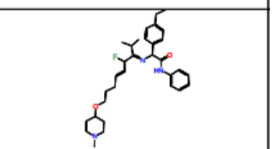
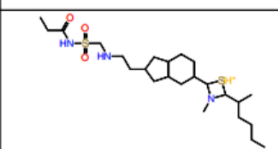
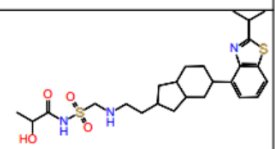
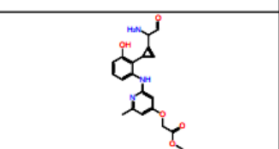
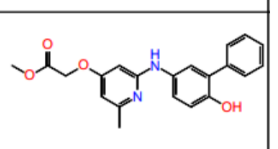
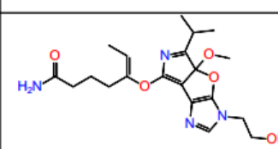
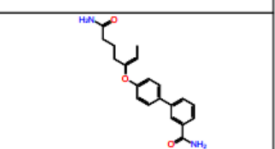
	
title: BACE2_HUMAN_76_460_0 : Unreasonable vina: -8.586	title: BACE2_HUMAN_76_460_0 : Reasonable vina: -9.854
	
title: F16P1_HUMAN_1_338_0 : Unreasonable vina: -8.173	title: F16P1_HUMAN_1_338_0 : Reasonable vina: -8.633
	
title: CAT_ECOLDX_1_219_0 : Unreasonable vina: -9.838	title: CAT_ECOLDX_1_219_0 : Reasonable vina: -10.164
	
title: DFPA_LOLVU_2_314_0 : Unreasonable vina: -7.208	title: DFPA_LOLVU_2_314_0 : Reasonable vina: -8.581
	
title: QPCT_HUMAN_33_361_0 : Unreasonable vina: -8.178	title: QPCT_HUMAN_33_361_0 : Reasonable vina: -9.527
	
title: KS6A3_HUMAN_41_357_0 : Unreasonable vina: -8.242	title: KS6A3_HUMAN_41_357_0 : Reasonable vina: -8.738
	
title: AROE_THET8_1_263_0 : Unreasonable vina: -8.741	title: AROE_THET8_1_263_0 : Reasonable vina: -8.794

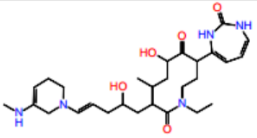
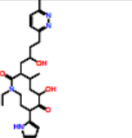
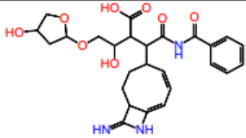
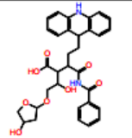
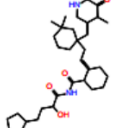
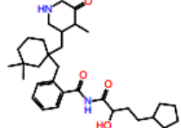
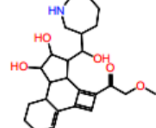
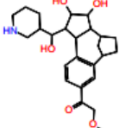
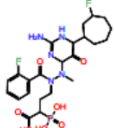
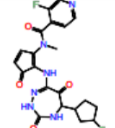
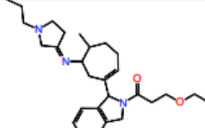
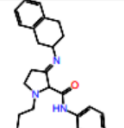
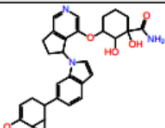
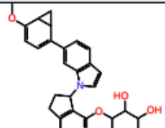
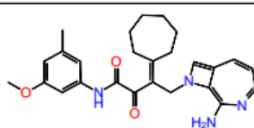
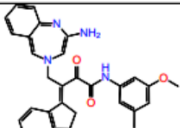
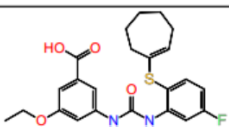
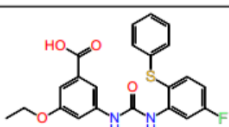
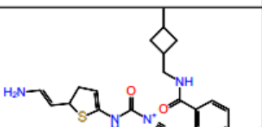
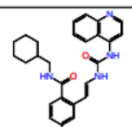
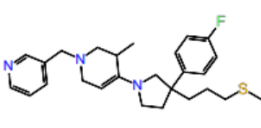
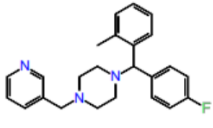
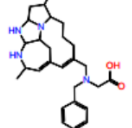
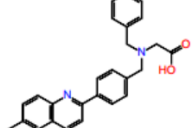
## Supporting molecule

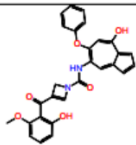
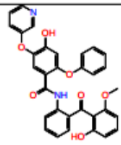
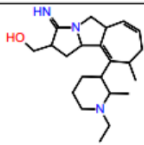
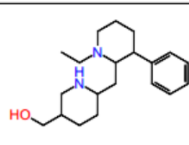
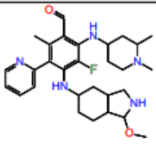
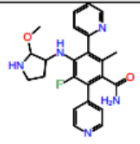
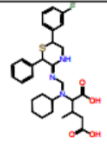
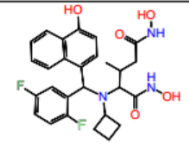
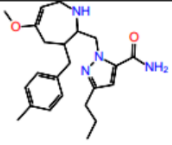
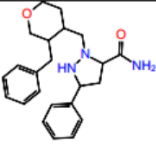
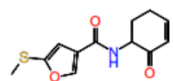
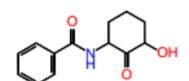
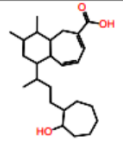
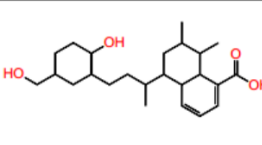
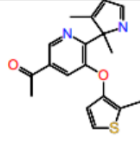
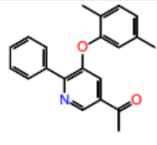
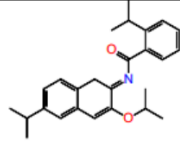
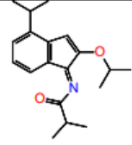
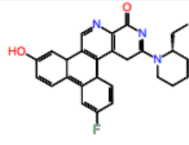
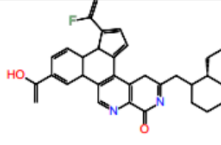
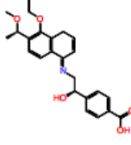
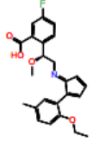
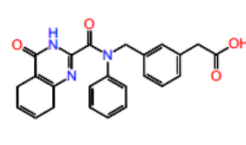
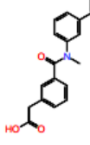
## CIDD output

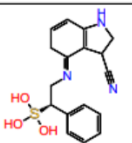
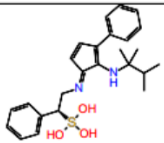
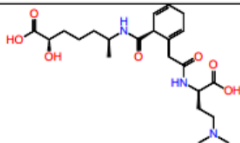
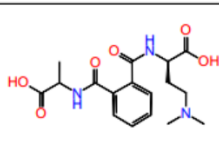
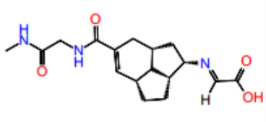
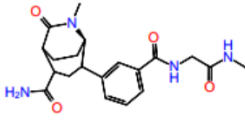
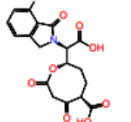
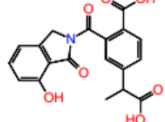
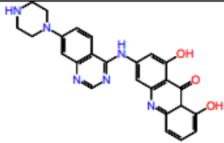
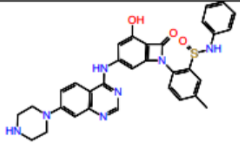
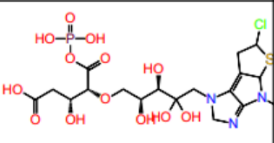
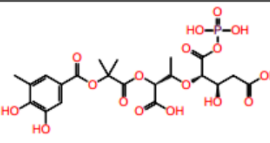
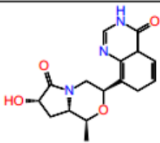
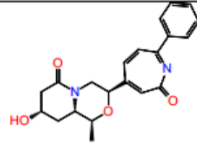
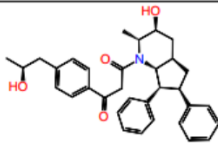
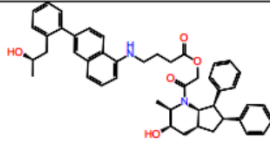
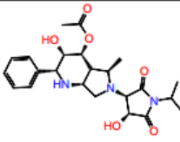
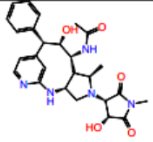
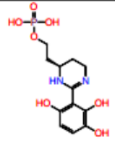
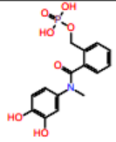
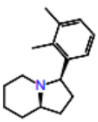
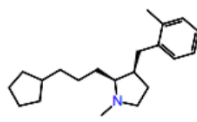
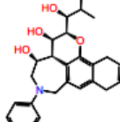
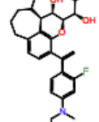
	
title: GRK4_HUMAN_1_578_0 : Unreasonable vina: -7.158	title: GRK4_HUMAN_1_578_0 : Reasonable vina: -8.93
	
title: CPXB_BACMB_2_464_0 : Unreasonable vina: -10.201	title: CPXB_BACMB_2_464_0 : Reasonable vina: -11.121
	
title: BSD_ASPTE_1_130_0 : Unreasonable vina: -7.492	title: BSD_ASPTE_1_130_0 : Reasonable vina: -8.786
	
title: RG1_RAUSE_1_513_0 : Unreasonable vina: -10.06	title: RG1_RAUSE_1_513_0 : Reasonable vina: -11.978
	
title: QPCT_HUMAN_33_361_0 : Unreasonable vina: -7.531	title: QPCT_HUMAN_33_361_0 : Reasonable vina: -8.356
	
title: GUX1_HYPJE_18_451_0 : Unreasonable vina: -7.25	title: GUX1_HYPJE_18_451_0 : Reasonable vina: -8.375
	
title: UPPS_ECOLDX_1_253_0 : Unreasonable vina: -7.288	title: UPPS_ECOLDX_1_253_0 : Reasonable vina: -8.315

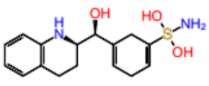
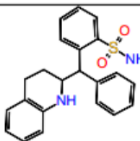
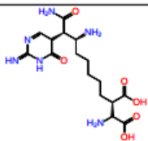
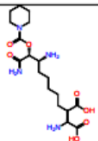
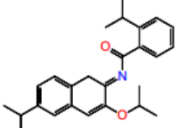
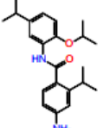
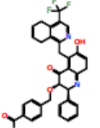
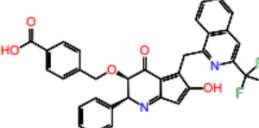
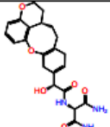
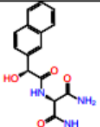
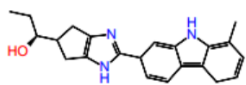
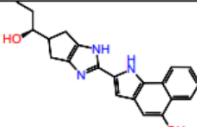
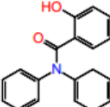
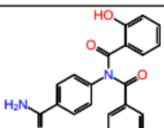
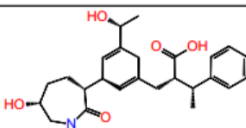
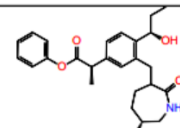
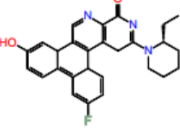
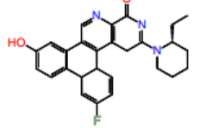
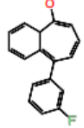
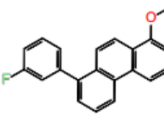
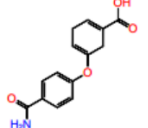
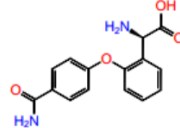
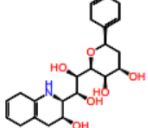
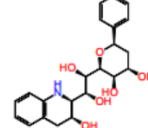
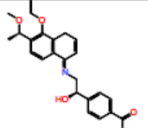
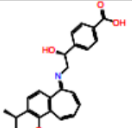
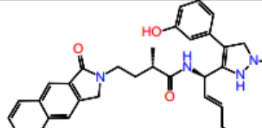
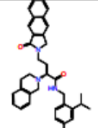


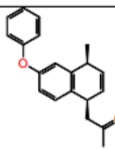
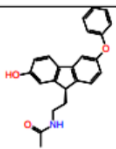
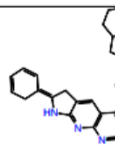
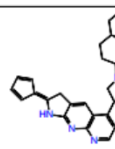
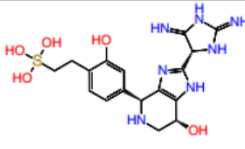
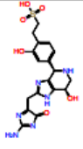
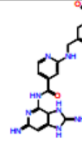
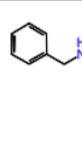
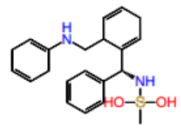
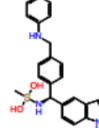
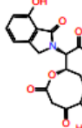
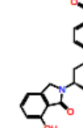
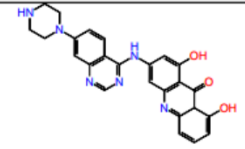
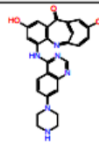
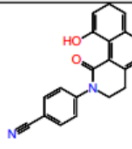
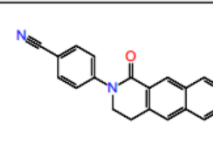
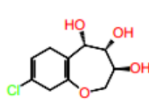
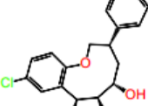
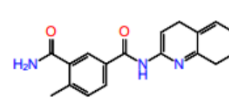
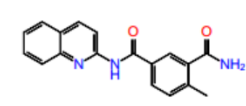
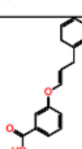
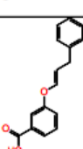
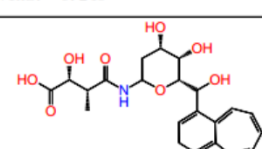
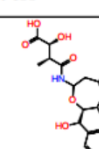
Supporting molecule	CIDD output	Supporting molecule	CIDD output
 title: CAT_ECCLX_1_219_0 : Unreasonable vina: -9.836	 title: CAT_ECCLX_1_219_0 : Reasonable vina: -11.246	 title: ATS5_HUMAN_262_480_0 : Unreasonable vina: -8.133	 title: ATS5_HUMAN_262_480_0 : Reasonable vina: -8.863
 title: NOS2_HUMAN_78_505_0 : Unreasonable vina: -10.504	 title: NOS2_HUMAN_78_505_0 : Reasonable vina: -11.006	 title: NOS2_HUMAN_78_505_0 : Unreasonable vina: -10.76	 title: NOS2_HUMAN_78_505_0 : Reasonable vina: -12.037
 title: BTRN_BACCI_2_250_0 : Unreasonable vina: -4.306	 title: BTRN_BACCI_2_250_0 : Reasonable vina: -11.729	 title: ACE_HUMAN_650_1230_0 : Unreasonable vina: -8.564	 title: ACE_HUMAN_650_1230_0 : Reasonable vina: -10.503
 title: ACE_HUMAN_650_1230_0 : Unreasonable vina: -9.498	 title: ACE_HUMAN_650_1230_0 : Reasonable vina: -10.987	 title: ACE_HUMAN_650_1230_0 : Unreasonable vina: -8.69	 title: ACE_HUMAN_650_1230_0 : Reasonable vina: -8.905
 title: AKT1_HUMAN_1_137_0 : Unreasonable vina: -11.185	 title: AKT1_HUMAN_1_137_0 : Reasonable vina: -11.293	 title: TBK1_HUMAN_1_303_0 : Unreasonable vina: -7.693	 title: TBK1_HUMAN_1_303_0 : Reasonable vina: -8.868
 title: BAPA_SPHXN_30_402_0 : Unreasonable vina: -7.681	 title: BAPA_SPHXN_30_402_0 : Reasonable vina: -8.683	 title: BAPA_SPHXN_30_402_0 : Unreasonable vina: -7.794	 title: BAPA_SPHXN_30_402_0 : Reasonable vina: -8.198

Supporting molecule	CIDD output	Supporting molecule	CIDD output
 <p>title: PHKG1_RABIT_6_296_ATPsite_0 : Unreasonable vina: -8.922</p>	 <p>title: PHKG1_RABIT_6_296_ATPsite_0 : Reasonable vina: -9.205</p>	 <p>title: BGL07_ORYSJ_25_504_0 : Unreasonable vina: -10.446</p>	 <p>title: BGL07_ORYSJ_25_504_0 : Reasonable vina: -10.592</p>
 <p>title: RG1_RAUSE_1_513_0 : Unreasonable vina: -10.484</p>	 <p>title: RG1_RAUSE_1_513_0 : Reasonable vina: -11.024</p>	 <p>title: DPP2_HUMAN_27_492_0 : Unreasonable vina: -9.855</p>	 <p>title: DPP2_HUMAN_27_492_0 : Reasonable vina: -11.224</p>
 <p>title: CD38_HUMAN_44_300_0 : Unreasonable vina: -8.72</p>	 <p>title: CD38_HUMAN_44_300_0 : Reasonable vina: -9.327</p>	 <p>title: PTGIS_HUMAN_20_500_0 : Unreasonable vina: -8.318</p>	 <p>title: PTGIS_HUMAN_20_500_0 : Reasonable vina: -9.448</p>
 <p>title: XANLY_BACGL_26_777_0 : Unreasonable vina: -9.053</p>	 <p>title: XANLY_BACGL_26_777_0 : Reasonable vina: -9.483</p>	 <p>title: PPIA_HUMAN_1_165_0 : Unreasonable vina: -8.777</p>	 <p>title: PPIA_HUMAN_1_165_0 : Reasonable vina: -10.083</p>
 <p>title: PPIA_HUMAN_1_165_0 : Unreasonable vina: -8.023</p>	 <p>title: PPIA_HUMAN_1_165_0 : Reasonable vina: -8.605</p>	 <p>title: HMD_METJA_1_358_0 : Unreasonable vina: -8.349</p>	 <p>title: HMD_METJA_1_358_0 : Reasonable vina: -9.593</p>
 <p>title: SQHC_ALIAD_1_631_0 : Unreasonable vina: -11.51</p>	 <p>title: SQHC_ALIAD_1_631_0 : Reasonable vina: -14.292</p>	 <p>title: KS6A3_HUMAN_41_357_0 : Unreasonable vina: -8.967</p>	 <p>title: KS6A3_HUMAN_41_357_0 : Reasonable vina: -11.101</p>

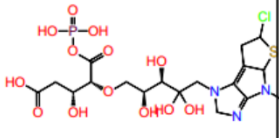
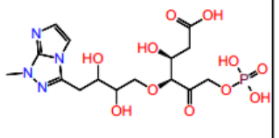
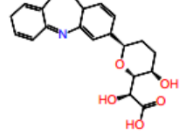
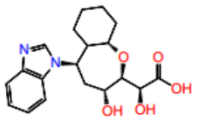
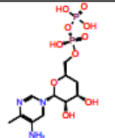
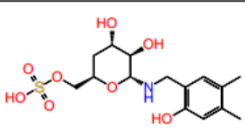
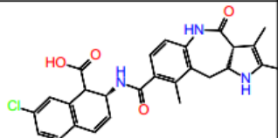
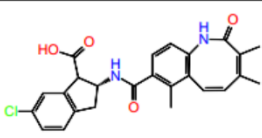
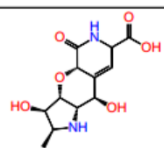
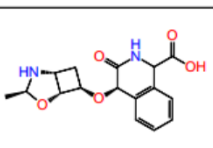
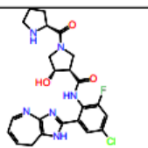
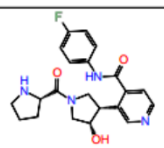
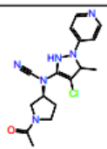
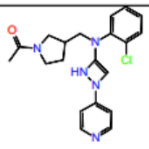
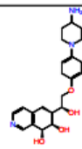
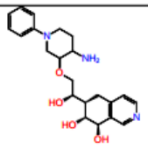
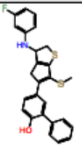
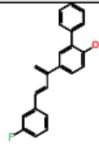
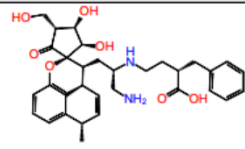
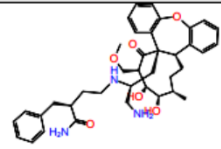
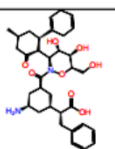
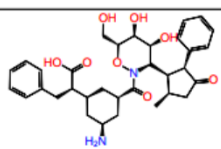
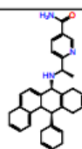
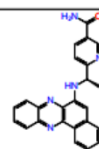
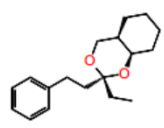
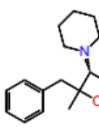
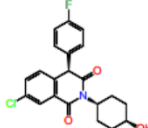
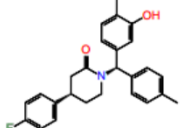
Supporting molecule	CIDD output	Supporting molecule	CIDD output
	 title: KS6A3_HUMAN_41_357_0 : Unreasonable vina: -9.414		 title: DYRK2_HUMAN_145_550_0 : Reasonable vina: -9.337
	 title: NR1H4_HUMAN_258_486_0 : Reasonable vina: -14.043		 title: BACE2_HUMAN_76_460_0 : Reasonable vina: -9.806
	 title: SDIA_ECOLI_1_171_0 : Unreasonable vina: -10.997		 title: TRAR_RHIRD_1_234_0 : Reasonable vina: -12.018
	 title: HDHA_ECOLI_1_255_0 : Unreasonable vina: -9.845		 title: UPPS_ECOLI_1_253_0 : Reasonable vina: -10.031
	 title: IDHP_HUMAN_40_452_0 : Reasonable vina: -10.368		 title: ABL2_HUMAN_274_551_0 : Reasonable vina: -10.776
	 title: AKT1_HUMAN_1_137_0 : Reasonable vina: -10.13		 title: : Reasonable vina: -10.893

Supporting molecule	CIDD output	Supporting molecule	CIDD output
 <p>title: MURA_ECOLI_1_419_catalytic_0 : Unreasonable vina: -8.295</p>	 <p>title: MURA_ECOLI_1_419_catalytic_0 : Reasonable vina: -9.241</p>	 <p>title: BGL07_ORYSJ_25_504_0 : Unreasonable vina: -8.187</p>	 <p>title: BGL07_ORYSJ_25_504_0 : Reasonable vina: -8.434</p>
 <p>title: BGL07_ORYSJ_25_504_0 : Unreasonable vina: -8.028</p>	 <p>title: BGL07_ORYSJ_25_504_0 : Reasonable vina: -9.632</p>	 <p>title: PAC_ECOLX_27_846_0 : Unreasonable vina: -8.228</p>	 <p>title: PAC_ECOLX_27_846_0 : Reasonable vina: -8.313</p>
 <p>title: PAC_ECOLX_27_846_0 : Unreasonable vina: -9.538</p>	 <p>title: PAC_ECOLX_27_846_0 : Reasonable vina: -10.042</p>	 <p>title: P2Y12_HUMAN_1_342_0 : Unreasonable vina: -8.514</p>	 <p>title: P2Y12_HUMAN_1_342_0 : Reasonable vina: -8.942</p>
 <p>title: EXG1_CANAL_41_438_0 : Unreasonable vina: -9.965</p>	 <p>title: EXG1_CANAL_41_438_0 : Reasonable vina: -10.569</p>	 <p>title: FKB1A_HUMAN_2_108_0 : Unreasonable vina: -7.899</p>	 <p>title: FKB1A_HUMAN_2_108_0 : Reasonable vina: -8.786</p>
 <p>title: CHIB_SERMA_1_499_0 : Unreasonable vina: -9.972</p>	 <p>title: CHIB_SERMA_1_499_0 : Reasonable vina: -10.354</p>	 <p>title: KS6A3_HUMAN_41_357_0 : Unreasonable vina: -7.827</p>	 <p>title: KS6A3_HUMAN_41_357_0 : Reasonable vina: -8.545</p>
 <p>title: SDIA_ECOLI_1_171_0 : Unreasonable vina: -10.933</p>	 <p>title: SDIA_ECOLI_1_171_0 : Reasonable vina: -11.339</p>	 <p>title: GUX1_HYPJE_18_451_0 : Unreasonable vina: -10.767</p>	 <p>title: GUX1_HYPJE_18_451_0 : Reasonable vina: -12.3</p>

Supporting molecule	CIDD output	Supporting molecule	CIDD output
			
title: HDHA_ECOLI_1_255_0 : Unreasonable vina: -8.511	title: HDHA_ECOLI_1_255_0 : Reasonable vina: -9.995	title: ODBB_THET8_1_324_0 : Unreasonable vina: -9.002	title: ODBB_THET8_1_324_0 : Reasonable vina: -9.322
			
title: IDHP_HUMAN_40_452_0 : Unreasonable vina: -8.039	title: IDHP_HUMAN_40_452_0 : Reasonable vina: -9.819	title: CPXB_BACMB_2_464_0 : Unreasonable vina: -9.196	title: CPXB_BACMB_2_464_0 : Reasonable vina: -12.034
			
title: NOS1_HUMAN_302_723_0 : Unreasonable vina: -9.495	title: NOS1_HUMAN_302_723_0 : Reasonable vina: -9.579	title: NOS1_HUMAN_302_723_0 : Unreasonable vina: -10.062	title: NOS1_HUMAN_302_723_0 : Reasonable vina: -10.305
			
title: CAT_ECOLX_1_219_0 : Unreasonable vina: -9.2	title: CAT_ECOLX_1_219_0 : Reasonable vina: -13.057	title: BSD_ASPTTE_1_130_0 : Unreasonable vina: -8.807	title: BSD_ASPTTE_1_130_0 : Reasonable vina: -9.501
			
title: ABL2_HUMAN_274_551_0 : Unreasonable vina: -10.702	title: ABL2_HUMAN_274_551_0 : Reasonable vina: -11.583	title: NQO1_HUMAN_2_274_0 : Unreasonable vina: -9.262	title: NQO1_HUMAN_2_274_0 : Reasonable vina: -10.424
			
title: BTRN_BACCI_2_250_0 : Unreasonable vina: -8.786	title: BTRN_BACCI_2_250_0 : Reasonable vina: -8.951	title: NAGZ_VIBCH_1_330_0 : Unreasonable vina: -7.206	title: NAGZ_VIBCH_1_330_0 : Reasonable vina: -8.307
			
title: AKT1_HUMAN_1_137_0 : Unreasonable vina: -10.1	title: AKT1_HUMAN_1_137_0 : Reasonable vina: -11.478	title: AKT1_HUMAN_1_137_0 : Unreasonable vina: -12.405	title: AKT1_HUMAN_1_137_0 : Reasonable vina: -13.048

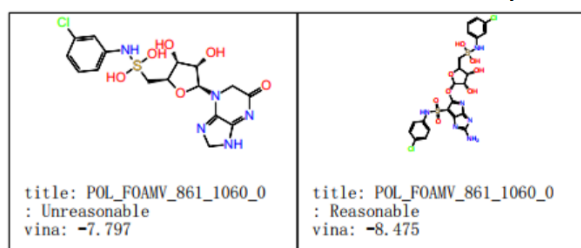
Supporting molecule	CIDD output	Supporting molecule	CIDD output
			
title: PA21B_PIG_23_146_0 : Unreasonable vina: -8.391	title: PA21B_PIG_23_146_0 : Reasonable vina: -10.029	title: PHKG1_RABIT_6_296_ATPsite_0 : Unreasonable vina: -10.937	title: PHKG1_RABIT_6_296_ATPsite_0 : Reasonable vina: -13.466
			
title: M3K14_HUMAN_321_678_0 : Unreasonable vina: -8.948	title: M3K14_HUMAN_321_678_0 : Reasonable vina: -9.001	title: M3K14_HUMAN_321_678_0 : Unreasonable vina: -9.44	title: M3K14_HUMAN_321_678_0 : Reasonable vina: -9.899
			
title: PTGIS_HUMAN_20_500_0 : Unreasonable vina: -7.955	title: PTGIS_HUMAN_20_500_0 : Reasonable vina: -9.193	title: PAC_ECOLX_27_846_0 : Unreasonable vina: -7.907	title: PAC_ECOLX_27_846_0 : Reasonable vina: -8.704
			
title: PAC_ECOLX_27_846_0 : Unreasonable vina: -9.272	title: PAC_ECOLX_27_846_0 : Reasonable vina: -9.421	title: TNKS2_HUMAN_948_1162_0 : Unreasonable vina: -10.215	title: TNKS2_HUMAN_948_1162_0 : Reasonable vina: -12.537
			
title: XANLY_BACGL_26_777_0 : Unreasonable vina: -6.991	title: XANLY_BACGL_26_777_0 : Reasonable vina: -8.994	title: PPIA_HUMAN_1_165_0 : Unreasonable vina: -9.243	title: PPIA_HUMAN_1_165_0 : Reasonable vina: -9.435
			
title: PPIA_HUMAN_1_165_0 : Unreasonable vina: -7.765	title: PPIA_HUMAN_1_165_0 : Reasonable vina: -8.447	title: P2Y12_HUMAN_1_342_0 : Unreasonable vina: -8.744	title: P2Y12_HUMAN_1_342_0 : Reasonable vina: -10.352



Supporting molecule	CIDD output	Supporting molecule	CIDD output
 <p>title: P2Y12_HUMAN_1_342_0 : Unreasonable vina: -8.31</p>	 <p>title: P2Y12_HUMAN_1_342_0 : Reasonable vina: -9.509</p>	 <p>title: EXG1_CANAL_41_438_0 : Unreasonable vina: -10.072</p>	 <p>title: EXG1_CANAL_41_438_0 : Reasonable vina: -10.17</p>
 <p>title: MENE_BACSU_2_486_0 : Unreasonable vina: -8.029</p>	 <p>title: MENE_BACSU_2_486_0 : Reasonable vina: -8.629</p>	 <p>title: SQHC_ALIAD_1_631_0 : Unreasonable vina: -9.519</p>	 <p>title: SQHC_ALIAD_1_631_0 : Reasonable vina: -12.291</p>
 <p>title: CHIB_SERMA_1_499_0 : Unreasonable vina: -7.389</p>	 <p>title: CHIB_SERMA_1_499_0 : Reasonable vina: -9.388</p>	 <p>title: SIR3_HUMAN_117_398_0 : Unreasonable vina: -10.258</p>	 <p>title: SIR3_HUMAN_117_398_0 : Reasonable vina: -10.419</p>
 <p>title: DYRK2_HUMAN_145_550_0 : Unreasonable vina: -7.898</p>	 <p>title: DYRK2_HUMAN_145_550_0 : Reasonable vina: -9.098</p>	 <p>title: NOS3_HUMAN_65_480_0 : Unreasonable vina: -9.821</p>	 <p>title: NOS3_HUMAN_65_480_0 : Reasonable vina: -10.535</p>
 <p>title: NR1H4_HUMAN_258_486_0 : Unreasonable vina: -8.974</p>	 <p>title: NR1H4_HUMAN_258_486_0 : Reasonable vina: -9.969</p>	 <p>title: BACE2_HUMAN_76_460_0 : Unreasonable vina: -9.302</p>	 <p>title: BACE2_HUMAN_76_460_0 : Reasonable vina: -9.947</p>
 <p>title: BACE2_HUMAN_76_460_0 : Unreasonable vina: -9.473</p>	 <p>title: BACE2_HUMAN_76_460_0 : Reasonable vina: -9.828</p>	 <p>title: SDIA_ECOLI_1_171_0 : Unreasonable vina: -8.889</p>	 <p>title: SDIA_ECOLI_1_171_0 : Reasonable vina: -13.779</p>
 <p>title: TRAR_RHIRD_1_234_0 : Unreasonable vina: -10.182</p>	 <p>title: TRAR_RHIRD_1_234_0 : Reasonable vina: -13.112</p>	 <p>title: TRAR_RHIRD_1_234_0 : Unreasonable vina: -9.69</p>	 <p>title: TRAR_RHIRD_1_234_0 : Reasonable vina: -15.856</p>

Supporting molecule

CIDD output



Supporting molecule

CIDD output

